INFN - Laboratori Nazionali di Frascati, May 1995
From: **The Second DaΦne Physics Handbook**[1]
Chapter 9: One Photon Initiated Processes
Eds. L. Maiani, G. Pancheri, N. Paver

Vector Meson Decays in Effective Chiral Lagrangians

A. Bramon
Grup de Física Teòrica, Universitat Autònoma de Barcelona,
08193 Bellaterra (Barcelona), Spain

A. Grau
Departamento de Física Teórica y del Cosmos,
Universidad de Granada, 18071 Granada, Spain
and
G. Pancheri
INFN, Laboratori Nazionali di Frascati, P.O.Box 13, I-00044 Frascati

Contents

[1]Supported by the INFN, by the EC under the HCM contract number CHRX-CT920026 and by the authors home institutions

1 Introduction

We give a brief description of some theoretical models which incorporate vector mesons in low energy effective lagrangians, namely the massive Yang-Mills approach, the Hidden Symmetry scheme and the conventional Vector Meson Dominance (VMD) model. We calculate a number of vector meson decays using the above schemes with and without implementation of chiral loop contributions. This is done for several processes of the anomalous and non-anomalous type, like $V^0 \to P^0\gamma$ and $V^0 \to P^0 P^0 \gamma$, with $V^0 = \rho, \omega, \phi$ and $P^0 = \pi^0, \eta$, some of which can be measurable at DAΦNE . We then turn to describe how one can introduce SU(3)-breaking in the vector-meson sector of effective chiral lagrangians incorporating vector-mesons (VM) as (hidden symmetry) gauge fields. We show that it is possible to consistently describe SU(3) breaking effects in the masses (M_V), couplings to the photon field ($f_{V\gamma}$) and to pseudoscalar pairs (g_{VPP}), pseudoscalar decay-constants (f_P) and charge radii ($< r_P^2 >$), in terms of just two parameters. A thorough description of all the above quantities is further improved when working in the context of Chiral Perturbation Theory (ChPT). We also show how to extend this procedure to the sector containing the VVP vertices related to the anomaly. An improved description of $VP\gamma$ and $P\gamma\gamma$ transitions is obtained.

2 Role played by VM in saturating the counterterms in ChPT

The inclusion of spin-1 mesons in effective chiral lagrangians has been largely discussed in the past and, with considerably renewed interest, during the last years. Indeed, traditional ideas associating spin-1 mesons with gauge bosons of local symmetries have been revisited and developed further. The so-called "massive Yang-Mills approach" and "hidden symmetry scheme" recently reviewed by Meissner [1] and Bando et al.[2] are two excellent and well detailed examples.

Conventional ChPT accounts for electro-weak and strong interactions of pseudoscalar mesons , P, in a perturbative series expansion in terms of their masses or four-momenta [3]. At lowest order in this expansion, the chiral lagrangian starts with the term

$$\mathcal{L}^{(2)} = \frac{f^2}{8} Tr(\mathcal{D}_\mu \Sigma \mathcal{D}^\mu \Sigma^\dagger) \tag{1}$$

where the pion decay constant $f = 132 MeV = f_\pi$ ($= f_K$, at this lowest-order level) and $\Sigma = \xi\xi = exp(2iP/f)$ with the matrix P given by

$$P = \begin{pmatrix} \frac{\pi^0}{\sqrt{2}} + \frac{\eta_8}{\sqrt{6}} + \frac{\eta_1}{\sqrt{3}} & \pi^+ & K^+ \\ \pi^- & -\frac{\pi^0}{\sqrt{2}} + \frac{\eta_8}{\sqrt{6}} + \frac{\eta_1}{\sqrt{3}} & K^0 \\ K^- & \bar{K}^0 & -\frac{2\eta_8}{\sqrt{6}} + \frac{\eta_1}{\sqrt{3}} \end{pmatrix} \tag{2}$$

where, for later convenience, the singlet term η_1 has been added to the conventional octet part (see Ametller's contribution to this Handbook). Electromagnetic interactions are contained in the covariant derivative

$$\mathcal{D}_\mu \Sigma = \partial_\mu \Sigma + ieA_\mu [Q, \Sigma] \tag{3}$$

where A_μ is the photon field (the extension to weak interactions being trivial) and Q is the quark-charge matrix $Q = diag(2/3, -1/3, -1/3)$. The mass degeneracy is broken via the additional mass term

$$\mathcal{L}_m^{(2)} = \frac{f^2}{8} Tr(\chi \Sigma^\dagger + \Sigma \chi^\dagger) \tag{4}$$

with χ containing the quark-mass matrix $M = diag(m_u, m_d, m_s)$ and transforming as a $(3, 3^*) + (3^*, 3)$ representation of $SU(3)_L \times SU(3)_R$. At this lowest order, ChPT essentially coincides with Current Algebra.

The next order piece in the chiral expansion (fourth order) contains one-loop corrections with vertices from (1) to (4) and a series of ten counterterms required to cancel loop divergencies [3]. Some of them, e.g.,

$$\mathcal{L}_9^{(4)} = -ieL_9 F_{\mu\nu} Tr(Q\ \mathcal{D}^\mu \Sigma\ \mathcal{D}^\nu \Sigma^\dagger + Q\ \mathcal{D}^\mu \Sigma^\dagger\ \mathcal{D}^\nu \Sigma) \tag{5}$$

are chiral-SU(3) symmetric, wheareas others, e.g.,

$$\mathcal{L}_5^{(4)} = \ L_5 Tr\left(\mathcal{D}_\mu \Sigma \mathcal{D}^\mu \Sigma^\dagger \left(\chi \Sigma^\dagger + \Sigma \chi^\dagger\right)\right) \tag{6}$$

break the symmetry as $\mathcal{L}_m^{(2)}$ in eq.(4). At this one-loop level, one obtains [3]

$$\frac{f_K}{f_\pi} = 1 + \frac{5}{4}\mu_\pi - \frac{1}{2}\mu_K - \frac{3}{4}\mu_\eta + \frac{8}{f^2}(m_K^2 - m_\pi^2) L_5(\mu) \tag{7}$$

where loop effects appear through the so-called chiral-logs $\mu_P = \dfrac{m_P^2}{16\pi^2 f^2}\ ln \dfrac{m_P^2}{\mu^2}$. Similarly, the pseudoscalar electromagnetic charge-radii are found to be [3]

$$\begin{aligned}
< r_{\pi^+}^2 > &= \frac{-1}{16\pi^2 f^2}\left(3 + 2\ ln\frac{m_\pi^2}{\mu^2} + ln\frac{m_K^2}{\mu^2}\right) + \frac{24}{f^2} L_9(\mu) \\
< r_{K^+}^2 > &= \frac{-1}{16\pi^2 f^2}\left(3 +\ ln\frac{m_\pi^2}{\mu^2} + 2\ ln\frac{m_K^2}{\mu^2}\right) + \frac{24}{f^2} L_9(\mu) \\
- < r_{K^0}^2 > &= < r_{\pi^+}^2 > - < r_{K^+}^2 > = \frac{1}{16\pi^2 f^2}\ ln\frac{m_K^2}{m_\pi^2}
\end{aligned} \tag{8}$$

where, again, the divergencies accompaning the chiral-logs are absorbed in one of the counterterms (or low-energy constants), L_9, appearing in $\mathcal{L}^{(4)}$.

The large number of low-energy constants one has to fix along the lines just discussed considerably reduces the predictive power of ChPT. For this reason, the attractive possibility that the values for those constants could be fixed assuming that they somehow parametrize the effects of the (so far ignored) exchange of the known meson resonances has been proposed [4] and successfully verified in many cases (see Chapter 3 in this Handbook for details). In most of them, particularly in processes involving the Wess-Zumino anomalous action, vector-mesons turn out to play the dominant role [5]. Their couplings to pseudoscalar plus photon states, as extracted from the experiments, saturate an important part of the above counterterms. Accurate effective lagrangians incorporating additional properties of vector mesons and further details on their dynamics could therefore be extremely useful not only as a self-contained effective theory but also as an auxiliary lagrangian fixing the counterterms in the ChPT context.

In order to illustrate the role played by vector mesons in saturating the counterterms, we consider the case [6] of the transition form factors controlling pseudoscalar radiative decays, i.e. $P \to \gamma\gamma^*$, where P=π^0, η, η'. The lowest order contribution to the corresponding amplitude F comes from the Wess-Zumino term $\mathcal{L}_{WZ}$ at order p^4 and is q^2 independent (q^2 being the mass of the off-shell photon). With the on-shell normalization

$$\Gamma(P^0 \to \gamma\gamma) = \frac{m_P^3}{64\pi}|F|^2 \tag{9}$$

the lowest order amplitude reduces to (see section 3 for details)

$$F = F_{LO}^{ChPT} = \frac{\alpha\sqrt{2}C_P}{\pi f_P} \tag{10}$$

where $C_\pi = 1, C_{\eta_8} = 1/\sqrt{3} = C_{\eta_1}/(2\sqrt{2})$ and all the decay constants f_P are the same at this order. Loop corrections modify the above result and introduce SU(3) breaking terms in the values for f_P. As in the non-anomalous case, cancellation of the loop divergences takes place through appropriate counterterms and the remaining finite contribution leads to

$$F_{LO}^{ChPT} \to F^{ChPT}(q^2) = F_{LO}^{ChPT}\left(1 + r_P b_L q^2\right) \tag{11}$$

with $r_\pi = 1, r_\eta = (2f_1 + f_8)/(2f_1 + 2f_8), r_{\eta'} = (f_1 - 4f_8)/(f_1 - 8f_8)$ (we have taken $sin\theta = -1/3$ for the η-η' mixing) and

$$b_L = -\frac{1}{24\pi^2 f^2}\left[1 + ln(m_K m_\pi/\mu^2)\right] \tag{12}$$

Fixing the scale μ at an average vector meson mass, i.e. $\mu^2 = (9m_\rho^2 + m_\omega^2 + 2m_\phi^2)/12$, the loop contribution gives $b_L = 0.32\ GeV^{-2}$, a value too small to reproduce the experimental data for the slope, as one can see in the pion case, where one has[7] $b_\pi = (1.79 \pm 0.14)\ GeV^{-2}$.

Let us now consider the direct contribution from the vector mesons to this process. It can be obtained from VMD as a sum over all the poles, i.e.

$$F^{VMD}(q^2) = \sum_V \frac{g_{PV\gamma}}{f_V}\frac{m_V^2}{m_V^2 - q^2}, \qquad F^{VMD}(0) = F_{LO}^{ChPT} \tag{13}$$

where the sum includes the contribution from the light vector mesons with SU(3) symmetric couplings to the photon, f_V, and to the meson-photon pair, $g_{VP\gamma}$. In the good SU(3) limit the contribution from vector mesons is the same for all the pseudoscalars, so that, expanding in powers of q^2/m_V^2, one can write

$$F(q^2) = F^{ChPT+VMD}(q^2) \simeq F_{LO}^{ChPT}\left[1 + (r_P b_L + b_V)q^2\right] \tag{14}$$

with $b_V = 1/\mu^2 = 1.46\ GeV^{-2}$. The entire q^2 dependence is parametrized in the low energy region through a single slope parameter $b_P = 1/\Lambda_P^2$ and the values thus obtained for Λ_P, summing together chiral loops and vector meson contributions, can be compared with experimental results with a very good agreement (see sect. 8.1 in this Handbook). Noticing that the vector meson contribution is quite larger (by almost a factor 5) than the one from the loops, it is clear that vector mesons are essential in reaching satisfactory agreement. It is also evident that there is essentially no space left for additional counterterm contributions, i.e. that vector mesons dominate or "saturate" the counterterms. Other examples of how vector mesons saturate the counterterms in the chiral lagrangian have been discussed in Chapters 3 and 8, as well as in ref. [8].

3 Different schemes for inclusion of Vector Mesons in effective lagrangians

In the previous section, we have discussed the implicit role played by vector mesons in chiral lagrangians, through saturation of the counterterm contributions. Beyond the very low energy region, where a lowest-order power expansion in p^2/μ^2 is sufficient, one may try to extend the validity of chiral lagrangians through the explicit introduction of vector meson fields. Two main lines have been developed, the massive Yang Mills (YM) approach proposed by Meissner [1] among other authors, and the Hidden Symmetry (HS) scheme proposed by Bando et al. [2]. In the former, spin-1 fields are introduced in the ungauged lagrangian through the usual covariant derivatives. Restricting, for simplicity of exposition, to the sole SU(2) fields, i.e. pions and ρ mesons, one starts with the usual lowest order lagrangian

$$\mathcal{L} = \frac{f^2}{8} tr\left(\partial_\mu \Sigma \partial^\mu \Sigma^\dagger\right) \tag{15}$$

and then makes the substitution

$$\partial_\mu \Sigma \to D_\mu \Sigma = \partial_\mu \Sigma + ig\left[\rho_\mu, \Sigma\right] \tag{16}$$

where $\Sigma = exp(2i\Pi/f)$ now contains only the pion field Π and ρ_μ is the ρ meson field. This results in the lowest order lagrangian

$$\begin{aligned}\mathcal{L}^{YM} &= \frac{f^2}{8} tr\left(D_\mu \Sigma D^\mu \Sigma^\dagger\right) = \\ &= ig\sqrt{2}\rho_\mu^0\left(\pi^+\partial^\mu\pi^- - \pi^-\partial^\mu\pi^+\right)\left[1 - \frac{1}{3f^2}\left(2\pi^0\pi^0 + 4\pi^+\pi^-\right)\right] \\ &\quad +2g^2\rho_\mu^0\rho^{0\mu}\pi^+\pi^- + \ldots\end{aligned} \tag{17}$$

where, for the sake of the present argument, we have shown only some terms involving interactions between neutral ρ mesons and pions. The gauge coupling constant g is determined by neutral ρ decay, $\Gamma(\rho^0 \to \pi^+\pi^-) = g^2 p_\pi^3/(3\pi M_\rho^2) = 151.2 \pm 1.2\ MeV$, to have the value $g = 4.2 \pm 0.1$. In the massive Yang Mills scheme, photonic interactions are then introduced through conventional Vector Meson Dominance, i.e. through the lagrangian

$$\mathcal{L}_{\rho\gamma} = -\sqrt{2} e f^2 g A^\mu \rho^0_\mu \tag{18}$$

which mediates all transitions between photons and matter fields. Applying this rule to the decay $\rho \to e^+e^-$, one obtains the relation $M_\rho^2 = 2g^2 f^2$ and $\Gamma(\rho \to e^+e^-) = 2\alpha^2 \pi M_\rho / 3g^2$. The experimental values $\Gamma(\rho^0 \to \pi^+\pi^-) = 151$ MeV and $\Gamma(\rho \to e^+e^-) = 6.74$ KeV are then fitted with $g = 4.0 \pm 0.2$. The dots in eq.(17) refer to further quadratic interactions between ρ and an even number of pion fields, but no mass terms for the vector mesons. This is to be contrasted with what happens in the lagrangian proposed by Bando et al.[2], in which the vector mesons enter explicitly as gauge fields of a "hidden" local symmetry of the chiral lagrangian, whereas the electro-weak gauge bosons are explicitly introduced through the usual covariant derivatives. A Higgs-like mechanism then generates the vector meson masses.

To wit, in the "hidden symmetry approach" of Bando et al.[2] the most general lagrangian containing pseudoscalar, vector and (external) electroweak gauge fields with the smallest number of derivatives, is given at the lowest order, by the linear combination $\mathcal{L}_A + a\mathcal{L}_V$, a being an arbitrary parameter, of the two SU(3) symmetric lagrangians

$$\begin{aligned} \mathcal{L}_A &= \frac{-f^2}{8} Tr\left(D_\mu \xi_L \cdot \xi_L^\dagger - D_\mu \xi_R \cdot \xi_R^\dagger\right)^2 \\ \mathcal{L}_V &= \frac{-f^2}{8} Tr\left(D_\mu \xi_L \cdot \xi_L^\dagger + D_\mu \xi_R \cdot \xi_R^\dagger\right)^2 \end{aligned} \tag{19}$$

The matrices ξ_L and ξ_R contain the pseudoscalars fields, P, and the unphysical (or compensator) scalar fields, σ, that will be absorbed to give a mass to the vector mesons

$$\xi_{L,R} = exp\left(i\sigma/f\right) \cdot exp\left(\mp iP/f\right) \tag{20}$$

The full covariant derivative is

$$D_\mu \xi_{L(R)} = \left(\partial_\mu - igV_\mu\right) \xi_{L(R)} + ie\xi_{L(R)} A_\mu \cdot Q \tag{21}$$

where only the photon field, A_μ, (but not its weak partners, as before) has been explicitly shown, and P and V now stand for the SU(3) octet and nonet matrices

$$P = \begin{pmatrix} \frac{\pi^0}{\sqrt{2}} + \frac{\eta}{\sqrt{6}} & \pi^+ & K^+ \\ \pi^- & -\frac{\pi^0}{\sqrt{2}} + \frac{\eta}{\sqrt{6}} & K^0 \\ K^- & \bar{K}^0 & -\frac{2\eta}{\sqrt{6}} \end{pmatrix} \qquad V = \begin{pmatrix} \frac{\rho^0}{\sqrt{2}} + \frac{\omega}{\sqrt{2}} & \rho^+ & K^{*+} \\ \rho^- & -\frac{\rho^0}{\sqrt{2}} + \frac{\omega}{\sqrt{2}} & K^{*0} \\ K^{*-} & \bar{K}^{*0} & \phi \end{pmatrix} \tag{22}$$

The lagrangian $\mathcal{L}_A + a\mathcal{L}_V$ can be reduced to the chiral lagrangian (1) for any value of the parameter a [2]. In fact, working in the unitary gauge ($\xi_L^\dagger = \xi_R = \xi = exp(iP/f)$) to eliminate the unphysical scalar fields and substituting the solution of the equation of motion for V_μ, the $\mathcal{L}_V$ part vanishes and $\mathcal{L}_A$ becomes identical to the non linear chiral lagrangian (1).

The "hidden symmetry" lagrangian $\mathcal{L}_A + a\mathcal{L}_V$ (19) can be easily seen to contain, among other things, a vector meson mass term, the pseudoscalar weak decay constants, the vector-photon conversion factor and the couplings of both vectors and photons to pseudoscalar pairs. The latter can be eliminated fixing $a = 2$, thus incorporating conventional vector-dominance in the electromagnetic form-factors of pseudoscalars. Returning, as before, to the simpler SU(2) case, for $\mathcal{L}_V$ one has

$$\begin{aligned}\mathcal{L}^{HS} &= \frac{a}{2} f^2 tr\left(g\rho_\mu - e\frac{\tau_3}{2}A_\mu + \frac{i}{2}\left(\xi\partial_\mu\xi^\dagger + \xi^\dagger\partial_\mu\xi\right) + ...\right)^2 \\ &= \frac{1}{2}M_\rho^2 tr(\rho_\mu\rho^\mu) - \sqrt{2}egf^2\rho_\mu^0 A^\mu + \sqrt{2}ig\rho_\mu^0\left(\pi^+\partial^\mu\pi^- - \pi^-\partial^\mu\pi^+\right) + ... \qquad (23)\end{aligned}$$

In the above equation, the constant a has been fixed to the value $a = 2$ in order to recover the relation between M_ρ and the ρ couplings, previously discussed. This lagrangian obviously reproduces all the lowest order results, as the previous one does, however it does not contain couplings between two or more ρ- mesons and an even number of pion fields.

It is not yet clear if these two lagrangians are fully equivalent or not. At first sight, processes involving one ρ meson and four or more pion fields could be used to discriminate between the two [9], since these processes could proceed through multiple ρ -pion interactions in the YM scheme, while not so in the HS approach. However, it has been pointed out that axial vector terms, not yet introduced in the above lagrangians, would probably play a role. This might render experimental discrimination rather difficult [10].

To the two schemes just discussed, one must also add the simplest and oldest of them all, i.e. conventional Vector Meson Dominance [11], in which all photon-pseudoscalar interactions proceed through vector meson fields with the same interaction lagrangian $\mathcal{L}_{V\gamma}$ seen before and the vector meson fields are introduced through the covariant derivatives in the free pion lagrangian $\mathcal{L} = \frac{1}{2}tr(\partial_\mu\Pi\partial^\mu\Pi)$. The lagrangian thus obtained

$$\mathcal{L}^{VMD} = igtr\left(\rho_\mu(\Pi\partial^\mu\Pi - \partial^\mu\Pi\Pi)\right) - \frac{g^2}{2}tr([\rho_\mu, \Pi])^2 \qquad (24)$$

contains the same $\rho - \pi\pi$ vertices as the previous two, but there are of course no multipion interactions, which in conventional VMD are basically frozen into the role played by the vector mesons.

After this brief introduction, we shall now discuss some vector meson decay processes which can be measured at DAΦNE , and in which the validity of the theoretical scenarios we have illustrated can be tested.

4 Anomalous processes like $V^0 \to P^0\gamma$

In this section, we present in detail the treatment of vector meson contributions to some anomalous processes of interest and show that in the anomalous sector, within the resonance saturation hypothesis, one can get unambiguous predictions for the renormalized parameters of the low energy effective Lagrangian. We shall start with the general discussion of the amplitude for $\pi^0 \to \gamma\gamma$, indicate its extension to the virtual photon case $\pi^0 \to \gamma\gamma^*$ in more detail than in the first section, discuss modifications due to counterterms and their saturation with vector mesons , and then illustrate the introduction in the chiral lagrangian of vector meson fields as from the Hidden Symmetry approach. The resulting lagrangian contains three parameters which we show to be related to the usual chiral perturbative counterterms. Examining processes like $\omega \to \pi^0\gamma$ with the photon on or off the masss shell, we are able to indicate a range of variability for these parameters and will then proceed to calculate the cross-section for the three processes $e^+e^- \to \pi^0\gamma, \eta\gamma, \pi^0\mu^+\mu^-$.

We focus our attention to the next-to-leading effective chiral Lagrangian describing the interaction of photons with pseudoscalars. Explicitly, the relevant part of the lowest-order anomalous Lagrangian is

$$\begin{aligned} \mathcal{L}_{WZ} &= -i\frac{e^2}{8\pi^2}\epsilon^{\mu\nu\alpha\beta}\partial_\mu A_\nu A_\alpha\ tr[(Q^2+\frac{1}{2}Q\Sigma Q\Sigma^\dagger)\partial_\beta\Sigma\Sigma^\dagger-(Q^2+\frac{1}{2}Q\Sigma^\dagger Q\Sigma) \\ &\quad \times\partial_\beta\Sigma^\dagger\Sigma]-\frac{e}{16\pi^2}\epsilon^{\mu\nu\alpha\beta}A_\mu\ tr[Q(\partial_\nu\Sigma\partial_\alpha\Sigma^\dagger\partial_\beta\Sigma\Sigma^\dagger-\partial_\nu\Sigma^\dagger\partial_\alpha\Sigma\partial_\beta\Sigma^\dagger\Sigma)]+... \end{aligned} \tag{25}$$

where the dots refer to non-photonic terms, irrelevant for our present purposes, and the whole nonet of pseudoscalar mesons (with the phenomenologically preferred η-η' mixing angle $\theta_P \simeq -\arcsin\ 1/3 \simeq -19.5°$) now appears in $\mathcal{L}_{WZ}$ through the matrix Σ defined in the first section.

¿From the first term in (25) one immediately deduces the amplitude for the $\pi^0 \to \gamma\gamma$ decay to order p^4, i.e.

$$A(\pi^0\to\gamma\gamma)=i\frac{\alpha\sqrt{2}}{\pi f}\epsilon^{\mu\nu\alpha\beta}\epsilon_\mu k_\nu\epsilon'_\alpha k'_\beta\,, \tag{26}$$

which successfully predicts $\Gamma(\pi^0\to\gamma\gamma)=\alpha^2m^3_{\pi^0}/(32\pi^3f^2)=7.6$ eV for $f=132$ MeV. Similarly, one obtains a good description of η, $\eta'\to\gamma\gamma$ decays as shown in ref.[12] for the above value of θ_P.

While this amplitude is finite, this result no longer holds when dealing with off-mass-shell photon(s), as in the $\gamma\gamma^*\to\pi^0$, η production or in the $\pi^0\to\gamma e^+e^-$, $\eta\to\gamma\mu^+\mu^-$ decay amplitudes. In these cases, diagrams like the ones in Fig.(1) give a contribution whose divergence is cancelled by a corresponding counterterm in the relevant order six lagrangian, i.e. [12]

$$\begin{aligned} \mathcal{L}^{(6)} &= i\epsilon^{\mu\nu\alpha\beta}F_{\alpha\beta}\partial^\lambda F_{\lambda\nu}\{B_1tr(Q^2\Sigma^\dagger\partial_\mu\Sigma-Q^2\Sigma\partial_\mu\Sigma^\dagger) \\ &\quad +B_2tr(Q\Sigma^\dagger Q\partial_\mu\Sigma-Q\Sigma Q\partial_\mu\Sigma^\dagger)\} \end{aligned} \tag{27}$$

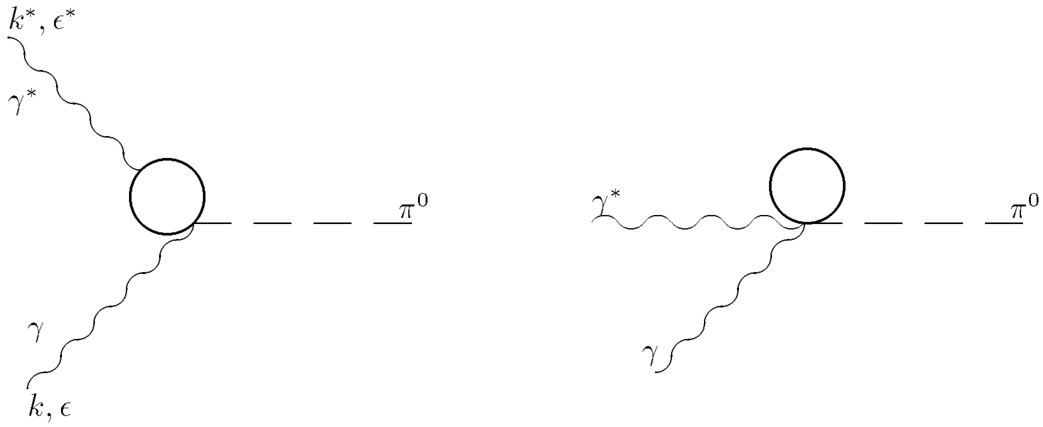

Figure 1: Loop diagrams contributing to $P \to \gamma\gamma^*$ processes at order p^6

where B_1 and B_2 are constants to be determined. Calling C_l and C^r the finite part of loop and counterterm corrections, the resulting amplitude is now written as [12]

$$A(\gamma\gamma^* \to P) = i\frac{\alpha\sqrt{2}C_P}{\pi f}\epsilon^{\mu\nu\alpha\beta}\epsilon_\mu k_\nu \epsilon^*_\alpha k^*_\beta \left[1 + C_l(\mu, k^{*2}) + C^r(\mu)k^{*2}\right], \tag{28}$$

where, $C_\pi = 1$, $C_{\eta_8} = 1/\sqrt{3}$, $C_{\eta_1} = 2\sqrt{2}/\sqrt{3}$ and, neglecting the small effects originated by the η_1 singlet part in the physical η wave function,

$$C_l(\mu, k^{*2}) = \frac{1}{48\pi^2 f^2}\left[k^{*2}\ log\frac{\mu^4}{m_\pi^2 m_K^2} + \frac{10}{3}k^{*2} + 4\ F(m_\pi^2, k^{*2}) + 4\ F(m_K^2, k^{*2})\right] \tag{29}$$

with $F(m^2, k^{*2})$ defined as

$$\begin{aligned} F(m^2, k^{*2}) &= m^2\left(1 - \frac{x}{4}\right)\sqrt{\frac{x-4}{x}}\ ln\frac{\sqrt{x}+\sqrt{x-4}}{-\sqrt{x}+\sqrt{x-4}} - 2m^2, & x = \frac{k^{*2}}{m^2} > 4 \\ F(m^2, k^{*2}) &= 2m^2\left(1 - \frac{x}{4}\right)\sqrt{\frac{4-x}{x}}\ arctg\sqrt{\frac{x}{4-x}} - 2m^2, & x \leq 4 \\ F(m^2, k^{*2}) &= -\frac{2k^{*2}}{3} & x \ll 1. \end{aligned} \tag{30}$$

The finite parts of the loop and counterterm corrections depend on the renormalization mass scale μ. This will be fixed around the ρ- and ω-meson masses, $\mu^2 \simeq m^2_{\rho,\omega} \equiv (m_\rho^2 + m_\omega^2)/2 \simeq 0.60$ GeV^2, which are the relevant ones in our case. Then eq.(29) for $k^{*2} \ll m^2_{\pi,K}$ reduces to

$$C_l(\mu, k^{*2}) \simeq \frac{1}{48\pi^2 f^2}\left(log\frac{\mu^4}{m_\pi^2 m_K^2} - 2\right)k^{*2} \equiv k^{*2}/\Lambda_l^2, \quad \text{with } \Lambda_l^{-2} \simeq 0.28\ \text{GeV}^{-2}. \tag{31}$$

As for the counterterm contribution, from eq.(27) one immediately has

$$C^r(\mu) = -\frac{4\pi}{3\alpha}(B_1 + B_2) \tag{32}$$

The numerical value of (32) can be fixed from experiments on $\pi^0 \to \gamma e^+ e^-$ decays [13] or (better) from a recent experiment on $\gamma^*\gamma \to \pi^0$ production through one (essentially) real photon and a virtual one [7]. The measured k^{*2}-dependence of the amplitude can be linearly parametrized in terms of a slope parameter b_{π^0}, i.e.

$$A(\gamma\gamma^* \to \pi^0) = i\frac{\alpha\sqrt{2}}{\pi f}\epsilon^{\mu\nu\alpha\beta}\epsilon_\mu k_\nu \epsilon^*_\alpha k^*_\beta \; \left[1 + b_{\pi^0} k^{*2}\right] \tag{33}$$

Using also (31) and (32) one has [7]

$$b_{\pi^0}(exp) = (1.79 \pm 0.14) \text{ GeV}^{-2} = \frac{1}{\Lambda_l^2} - \frac{4\pi}{3\alpha}(B_1 + B_2) \tag{34}$$

By comparig this experimental result with the contribution from the loops (28), the counterterms contribution turns out to be dominant and given by

$$B_1 + B_2 = -(1.13 \pm 0.11)\frac{\alpha}{\pi} \text{ GeV}^{-2} = -(0.68 \pm 0.07)\frac{\alpha}{\pi m^2_{\rho,\omega}} \tag{35}$$

Similarly, a single measurement using $\eta \to \mu^+\mu^-\gamma$ leads to $b_\eta(exp) = (1.9 \pm 0.4)$ GeV^{-2}, thus confirming eqs.(34) and (35) (see Ametller's contribution to this Handbook).

The experimental results just described, and their parameterization in terms of $B_1 + B_2$, can now be used to test the saturation hypothesis of the counterterms by resonance exchange. Let us introduce in this context the whole nonet of vector mesons, V, as gauge bosons of the HS-model of Bando and collaborators [14, 2]. At order p^6, the relevant lagrangian (which can be found in ref. [12]) can be written as a linear combination of three independent terms with coefficients a_1, a_2, a_3. As it turns out, only terms proportional to the constants a_2 and a_3 are relevant to the processes we are interested here, while all three enter into the study of a process like $\omega \to 3\pi$, discussed in refs.[15, 16]. Including also the first term from $\mathcal{L}_{WZ}$ (25), the pieces of the whole Lagrangian relevant to $P\gamma\gamma$, $VP\gamma$ and VVP vertices are written as

$$\begin{aligned}
\mathcal{L}_{P\gamma\gamma} &= \left(\frac{3}{4\pi^2} + 8a_3\right)\frac{e^2}{f}\epsilon^{\mu\nu\alpha\beta}\partial_\mu A_\nu \partial_\alpha A_\beta \; tr(Q^2 P) \\
\mathcal{L}_{VP\gamma} &= (a_2 - 2a_3)\frac{2eg}{f}\epsilon^{\mu\nu\alpha\beta}\partial_\mu A_\nu \; tr(Q(\partial_\alpha V_\beta P + P\partial_\alpha V_\beta)) \\
\mathcal{L}_{VVP} &= -4a_2\frac{g^2}{f}\epsilon^{\mu\nu\alpha\beta} \; tr(\partial_\mu V_\nu \partial_\alpha V_\beta P),
\end{aligned} \tag{36}$$

Vector meson mass terms and standard $V\gamma$ couplings appear in the lagrangian

$$\mathcal{L}_V = f^2 tr(g^2 V_\mu V^\mu - 2egQA_\mu V^\mu + ...) = \frac{1}{2} m_V^2 tr(V_\mu V^\mu) + \mathcal{L}_{V\gamma} \tag{37}$$

with the constants g and f satisfying the relations $g = m_{\rho,\omega}/\sqrt{2}f \simeq 4.15$ and the lagrangian $\mathcal{L}_{V\gamma} = -em_V^2 A^\mu \left(\frac{\rho_\mu^0}{f_\rho} + \frac{\omega_\mu}{f_\omega} + \frac{\phi_\mu}{f_\phi}\right)$ generalizing eq.(18) with

$$f_\rho = \frac{1}{3} f_\omega = -\frac{\sqrt{2}}{3} f_\phi = \sqrt{2} g \tag{38}$$

The above contributions to the lagrangian are such that only the first term in $\mathcal{L}_{P\gamma\gamma}$, i.e. the first term in $\mathcal{L}_{WZ}$, contributes to the $P\gamma\gamma$ amplitude for real photons. Indeed once the $V\gamma$ transition (37) is used in eq.(36) there is a cancellation of all $a_{2,3}$ dependent terms and one recovers the results of eq.(26). The $a_{2,3}$ dependence appears when dealing with vertices such as $\omega\pi^0\gamma$, $\rho\eta\gamma$ or $\pi^0\gamma\gamma^*$, $\eta\gamma\gamma^*$, where the virtual photon introduces also a k^{*2}-dependence through the vector meson form-factor $m_{\omega,\rho}^2/(m_{\omega,\rho}^2 - k^{*2})$. Expanding in powers of $k^{*2}/m_{\omega,\rho}^2$ and retaining up to the second term, we can now compare the vector meson contributions from the above lagrangian (given in terms of $a_{2,3}$) with the $B_{1,2}$ coefficients in $\mathcal{L}^{(6)}$, eq.(27) . As shown in [12], one easily obtains

$$\mid B_1 + B_2 \mid_{VM} = 2\pi^2 \mid a_2 + 2a_3 \mid \frac{\alpha}{\pi m_{\rho,\omega}^2} \tag{39}$$

The actual numerical values for the above constants can be deduced from the experimental data relative to a $VP\gamma$ process like the decay $\omega \to \pi^0\gamma$. The measured width $\Gamma(\omega \to \pi^0\gamma) = (720 \pm 50)$ keV $\simeq 9\ \Gamma(\rho \to \pi\gamma)$ [13] leads to

$$2\pi^2 \mid a_2 + 2a_3 \mid \frac{\alpha}{\pi m_{\rho,\omega}^2} = (0.73 \pm 0.02) \frac{\alpha}{\pi m_{\rho,\omega}^2} \tag{40}$$

in good agreement with (35), thus confirming the resonance saturation hypothesis for the counterterms, $B_1 + B_2 \simeq (B_1 + B_2)_{VM}$.

Let us now discuss the relationship between the above lagrangians eqs.(36-37) and the vector meson dominance model, in which no direct coupling between pseudoscalar mesons and photons appears. This result is easily obtained with the following choice of parameters a_2 and a_3

$$a_2 = 2a_3 = -3/16\pi^2 \tag{41}$$

which eliminates all direct $P\gamma\gamma$ and $VP\gamma$ vertices in the Lagrangian (36). The relative decay vertices are then exclusively generated by the $\mathcal{L}_{VVP}$ term and $V\gamma$ conversion(s) from $\mathcal{L}_{V\gamma}$ as in conventional VMD, indicating the consistency of the latter with the model of Bando et al.[14, 2] for the above choice of the parameters a_2 and a_3. However, the agreement between eq.(35) and eqs.(39)and (40), which confirms the saturation hypothesis for the Bando model, does not fix the individual values of a_2 and a_3, but only the sum $|a_2 + 2a_3|$. The choice

$$a_2 + 2a_3 = -3/8\pi^2\,, \tag{42}$$

can then be adopted to include both the VMD conventional model, for which eq.(41) is satisfied, as well as deviations from this model through $a_2 \neq 2a_3$, while still satisfying eq.(40).

The possibility of deviations from VMD has been discussed in the related context of $\gamma^* \to PPP$ transitions[15]. Other informations can be extracted from experimental data on the decays $\omega \to \pi^0\gamma^* \to \pi^0\mu^+\mu^-$ [17] where the k^{*2}-dependence has been parametrized in terms of the usual e.m. transition form-factor $F_\omega \equiv \Lambda^2/(\Lambda^2 - k^{*2})$ (see Ll.Ametller in this Handbook). The data can be fitted with $\Lambda_{exp} = 0.65 \pm 0.03\ GeV$ and seem to indicate a deviation from the usual vector meson dominance, for which one would have chosen $\Lambda_{VMD} = m_{\rho,\omega} = 0.768\ GeV$. Such discrepancy can easily be explained in terms of the Lagrangians (36) and (37), which imply a form-factor given by

$$1 + \frac{2a_2}{(a_2 + 2a_3)} \frac{k^{*2}}{m_\rho^2} + ... \tag{43}$$

Comparing eq.(43) with $1 + k^{*2}/\Lambda_{exp}^2 + ...$, we see that experimental data imply $a_2 > 2a_3$ and, up to this order, a good choice seems to be $a_2 = 4.6\ a_3$. This is however not a completely unambiguous choice. If one is willing to extend this formalism to higher k^{*2}, the data [17] tend to prefer values of a_2 somewhat larger than $5a_3$, as one can see from Fig.(2), where we plot the fits for the k^{*2}-dependence of the form factor in $\omega \to \pi^0\gamma^*$ for the experimental case and two different choices of the parameters.

We see that we can adopt

$$a_2 = 6a_3 = -9/32\pi^2, \qquad a_2 + 2a_3 = -3/8\pi^2 \tag{44}$$

as a compromise which represents an interesting alternative to the VMD values (41).

Apart from giving a reasonable description of the $\omega \to \pi^0\mu^+\mu^-$ data, the values (44) are also in the preferred region in order to account for the data on the $\omega \to \pi^+\pi^-\pi^0$. This has been discussed in detail in refs.[15, 16], and the result can be summarized in Fig.(3), where values of the parameters a_1 and a_2 consistent with experimental data are plotted. The branching ratios for $\omega \to \pi^+\pi^-\pi^0$ and $\omega \to \pi^0\gamma$ fix a region in the a_1, a_2, a_3 parameter space, represented by the ellipse. The point B on the ellipse corresponds to the value in eq.(44) extracted from the process $\omega \to \pi^0\mu^+\mu^-$. Notice that these values of the parameters a_i, which imply a deviation from pure VMD, find a partial confirmation in recent analyses of the $\omega \to \pi^0\mu^+\mu^-$ form-factor in the lattice [18].

To summarize, we have discussed the relationship between conventional VMD, counterterm contributions in chiral perturbation theory and a possible model for introduction of vector mesons in the chiral lagrangian to saturate the counterterms. To clarify some of the issues involved, such as the presence of a possible clear deviation from VMD, we now proceed to calculate the production cross-sections for the reactions $e^+e^- \to \pi^0\gamma, \eta\gamma$ and $e^+e^- \to \pi^0 l^+ l^-$ which can be measured at DAΦNE and might improve the whole situation and contribute to fix the value of the ChPT counterterms or the $a_{2,3}$ parameters.

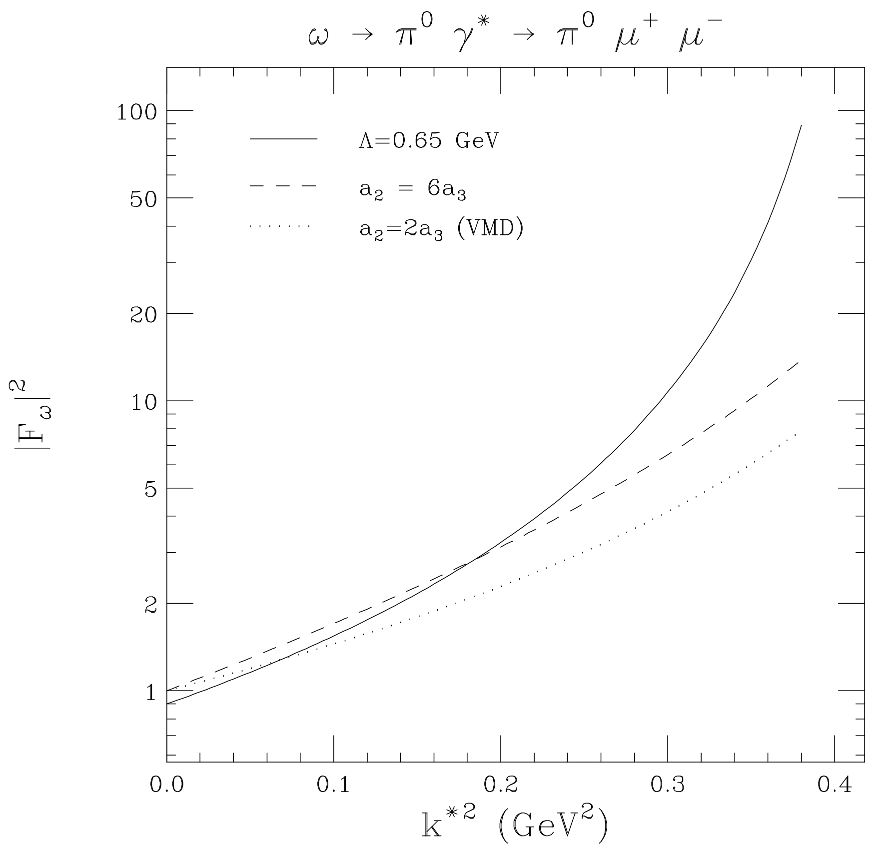

Figure 2: Fits to the k^{*2}-dependence of the form-factor in $\omega \to \pi^0\gamma^*$. The data (not shown) are compatible with the solid and dashed lines but not with VMD .

4.1 Calculation of cross-sections for $e^+e^- \to P\gamma, P\gamma^*$ at DAΦNE

The $e^+e^- \to \pi^0\gamma$ cross section at lowest order is obtained from $\mathcal{L}_{WZ}$ in eq.(25) and turns out to be

$$\sigma^{LO}_{e^+e^-\to\pi^0\gamma}(s) = \frac{\alpha^3}{12\pi^2 f^2}(1 - m^2_{\pi^0}/s)^3, \tag{45}$$

where s is the square of the total CM energy and $\alpha^3/(12\pi^2 f^2) = 0.0734$ nb. This lowest order cross section is shown (dotted line) in Fig.(4).

Next order corrections in ChPT include the effects of loops and counterterms as in eq.(28). For the latter, the resonance saturation assumption implies $C^r(\mu \simeq m_{\rho,\omega}) = 1/m^2_{\rho,\omega}$, thus increasing the lowest order amplitude up to a 60% at $E = \sqrt{s} = 0.6$ GeV as also shown (dashed line) in Fig.(4). The associated loop corrections are given by $C_l(\mu, s)$ in eq.(29). These loop corrections are considerably smaller than those coming from the

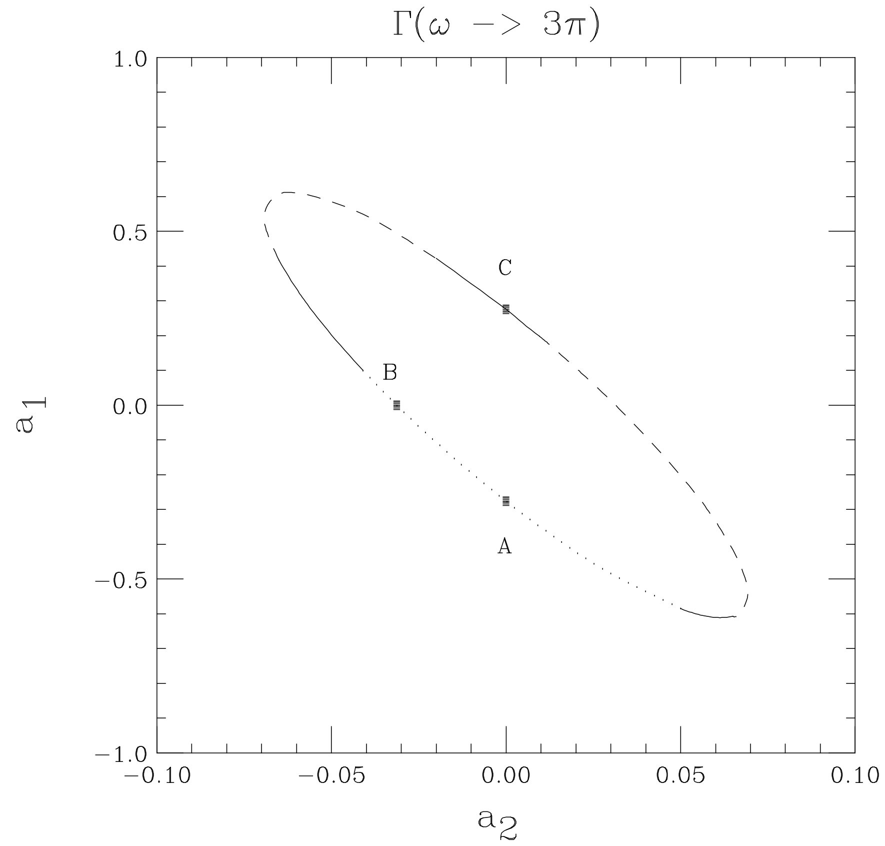

Figure 3: The ellipse defines the values of parameters a_1 and a_2 which give the correct width for the $\omega \to 3\pi$ within one (dots), two (full) or more (dashes) standard deviations from the data for $e^+e^- \to 3\pi$ cross-section near the ω peak. The choices A and C are discussed in [15].

corresponding counterterms (around a 15% in the amplitude) and slightly increase the $e^+e^- \to \pi^0\gamma$ cross-section, as shown (dot-dashed line) in Fig.(4). This curve represents the full ChPT prediction at next-to-leading order for $e^+e^- \to \pi^0\gamma$ and is expected to reproduce future data in the low energy region.

Around the resonance masses the cross-section is quite different as indicated by the value at the ω-peak [20] $\sigma_{e^+e^-\to\pi^0\gamma}(s = m_\omega^2) = 152 \pm 13$ nb, shown with error bars in Fig.(4). Attempts to improve the situation in ChPT would imply the evaluation of higher order loop corrections and the corresponding counterterms. In general and for values of $\mu \sim m_{\rho,\omega}$, next order loop corrections in ChPT are found to be around 10-20% of the preceding order amplitude, smaller than those coming from other uncertainties in our model and the values of its parameters. By contrast, corrections coming from counterterms have been shown to be larger than the ones from the loops and the evaluation of higher-order

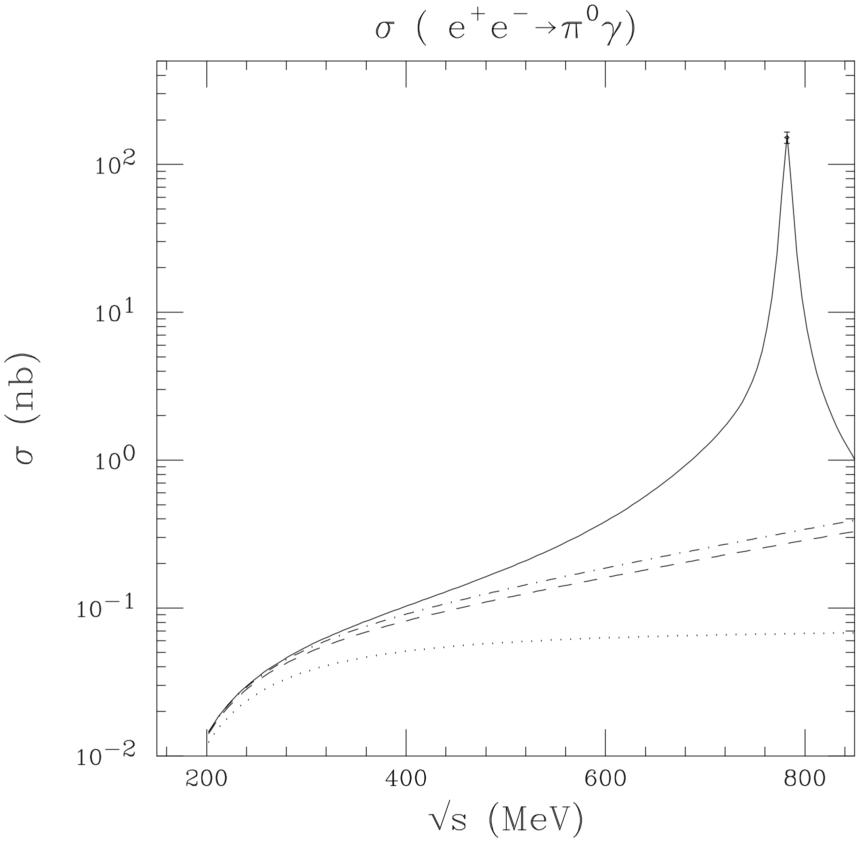

Figure 4: Cross-section for $e^+e^- \to \pi^0\gamma$ as a function of the total CM energy : lowest order result (dots), including counter-term contributions at the next order (dashes), full ChPT prediction (with loop and counterterm corrections) at next-to leading order (dot-dashes) and the "all-order" result (full line).

ones, under our assumption of resonance saturation, is trivial. As before, the introduction of the whole vector-meson form-factor $m^2_{\rho,\omega}/(m^2_{\rho,\omega} - s)$ (instead of its truncated series $1 + s/m^2_{\rho,\omega}$) represents an "*all-order*" estimate of our resonance dominated counterterms. Taking into account the physical finite widths of the ρ and ω mesons, this amounts to write

$$\begin{aligned} \sigma_{e^+e^-\to\rho,\omega\to\pi^0\gamma}(s) &= \frac{\alpha^3}{12\pi^2 f^2}(1 - m^2_{\pi^0}/s)^3 \mid C_l(\mu = m_{\rho,\omega}, s) + \frac{1}{2}P_\rho(s) + \frac{1}{2}P_\omega(s) \mid^2 \\ P_V(s) &\equiv m_V^2/(m_V^2 - s - i\sqrt{s}\Gamma_V), \qquad V = \rho^0, \omega \end{aligned} \tag{46}$$

to first order in the loop corrections. The corresponding prediction is also shown (solid line) in Fig.(4). The agreement at the ω-peak (161 nb vs 152$\pm$13 nb from experiment [20]) is essentially a consequence of having used $a_2 + 2a_3 = -3/8\pi^2$, and $\Gamma_{\omega\to all} = 8.43 \pm 0.10$ MeV and $BR(\omega \to \pi^0\gamma) = (8.5\pm0.5)\%$ [13], quite close to 8.4$\pm$0.1 MeV and (8.88$\pm$0.62)%

as measured in [20] from the $e^+e^- \to \omega \to \pi^0\gamma$ cross-section at the ω peak. Near this peak the ω-contribution is obviously dominant, but at lower energies, loop effects, counterterms and the ρ resonance curve represent a substantial fraction of the total cross-section.

The $e^+e^- \to \eta\gamma$ cross-section can be analyzed along the same lines. Eq.(46) becomes

$$\sigma_{e^+e^- \to \rho,\omega,\phi \to \eta\gamma}(s) = \frac{8\alpha^3}{(9\pi)^2 f^2}\left(1 - \frac{m_\eta^2}{s}\right)^3 |C_l(\mu, s) + \frac{9}{8}P_\rho(s) + \frac{1}{8}P_\omega(s) - \frac{1}{4}P_\phi(s)|^2 \tag{47}$$

and the various contributions arising from this expression have been plotted in Fig.(5), with the same notation employed for Fig.(4). The interference effects among the various

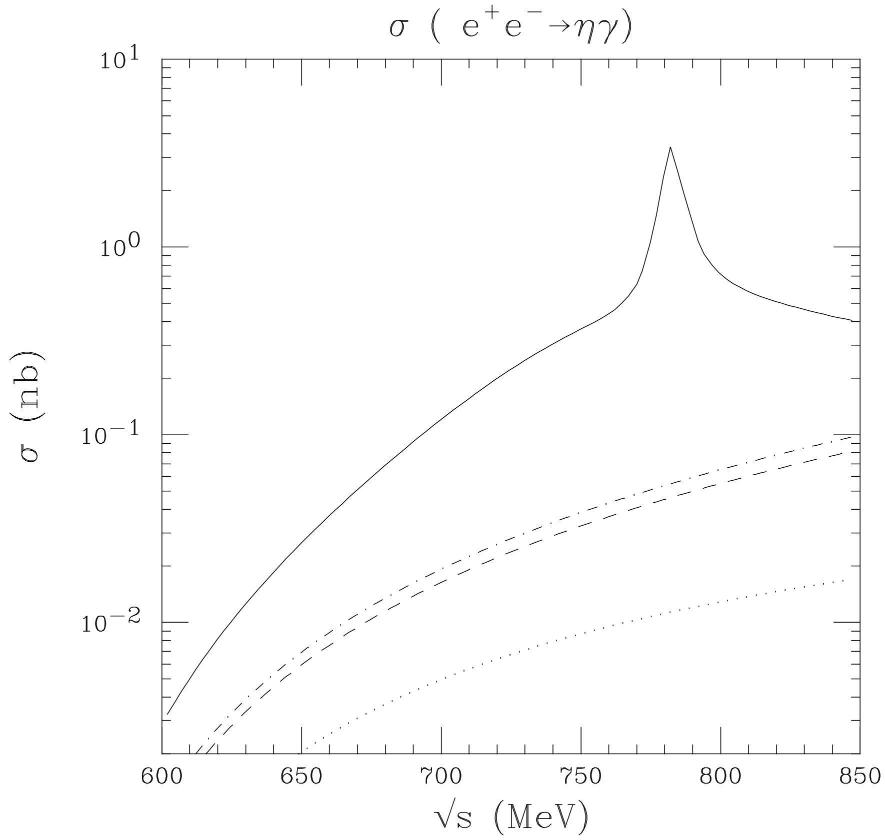

Figure 5: Cross-section for $e^+e^- \to \eta\gamma$ as a function of the CM energy, distinguishing different contributions near and around the omega peak from lowest order(dots), counterterms (dashes) and chiral loops (dotdashes).

terms are now important even on the ω-peak. Experimental data for $e^+e^- \to \eta\gamma$ in this energy region are known [20] but affected by large error bars.

Turning now to the $e^+e^- \to \pi^0\gamma^*$ transition, *i.e.*, allowing for the final state photon to be also off-mass-shell ($k^{*2} > 0$) as in $e^+e^- \to \pi^0 l^+ l^-$, one gets

$$\sigma_{e^+e^-\to\rho,\omega\to\pi^0\gamma^*}(s,k^{*2}) = \frac{\alpha^3}{12\pi^2 f^2}\left(1-\frac{(m_\pi+\sqrt{k^{*2}})^2}{s}\right)^{3/2}\left(1-\frac{(m_\pi-\sqrt{k^{*2}})^2}{s}\right)^{3/2}$$
$$\left[\left(1+\frac{2a_2}{a_2+2a_3}\frac{k^{*2}}{m_{\rho,\omega}^2-k^{*2}}\right)\frac{P_\rho(s)+P_\omega(s)}{2} + \left(1-\frac{2a_2}{a_2+2a_3}\right)\frac{k^{*2}}{m_{\rho,\omega}^2-k^{*2}}\right.$$
$$\left. +C_l(\mu,s)+C_l(\mu,k^{*2})\right]^2 \tag{48}$$

Eq.(48) leads to the $e^+e^- \to \pi^0\mu^+\mu^-$ cross-section plotted in Fig.(6) for $a_2+2a_3 = -3/8\pi^2$ and $a_2 = 6a_3$, $2a_3$ and 0 (dashed, solid and dotted lines). One obtains an ω-peak cross-section $\sigma_{e^+e^-\to\pi^0\mu^+\mu^-}(s=m_\omega^2) = 0.182$, 0.147 and 0.090 nb, respectively. The corresponding experimental value 0.164 ± 0.040 nb [20, 17] favours the first two possibilities but new experiments could contribute to clarify the situation discriminating among the different ratios a_2/a_3. This is not the case for the $e^+e^- \to \pi^0 e^+e^-$ cross-section (also shown in Fig.(6)) where the predictions for different values of a_2/a_3 are quite similar due to the dominance of small k^{*2} values which reduces the sensitivity on a_2/a_3 as seen in eq.(48). Moreover, for this particular process and well below the resonance region one could expect non-negligible contributions coming from the scattering channel $e^+e^- \to e^+e^-\gamma^*\gamma^* \to e^+e^-\pi^0$ with two spacelike photons [19].

In summary, $e^+e^- \to \pi^0\gamma$, $\eta\gamma$ and $e^+e^- \to \pi^0\mu^+\mu^-$ cross-sections at low energy seem particularly interesting to test the saturation of the ChPT counterterms by resonances, which in this case are expected to be the well-known ρ^0 and ω vector-mesons.

5 Non-anomalous processes like $V^0 \to P^0P^0\gamma$

In this section, we study the general process $V^0 \to P^0P^0\gamma$ both within the framework of pure VMD as well as including chiral loop contributions. It is important to have as precise as possible an estimate for these proceses, because they contribute to the background to physics reactions like $\phi \to f_0/a_0\gamma$ or to CP violation measurements, as it is the case for $\phi \to K^0\bar{K}^0\gamma$.

We start with the amplitude for the general process within the framework of Vector Meson Dominance (VMD). We find some discrepancies in the literature and update the results.

Subsequently, we look into the possibility that chiral loops may be relevant to the calculation of these processes, even at some relatively high energies, like around the ϕ-mass region. This attempt to extend ChPT to radiative vector-meson decays, $V^0 \to P^0P^0\gamma$, indicates that the effects of (chiral) loops may be important, at least in some cases [21]. Unambiguous predictions are then given for $\phi \to \pi^0\pi^0\gamma$, $\pi^0\eta\gamma$, $\rho \to \pi^0\pi^0\gamma$ and other processes of interest. The relation of ChPT amplitudes to the VMD ones is discussed in terms of the (VM-)resonance saturation of counterterms in the chiral lagrangian.

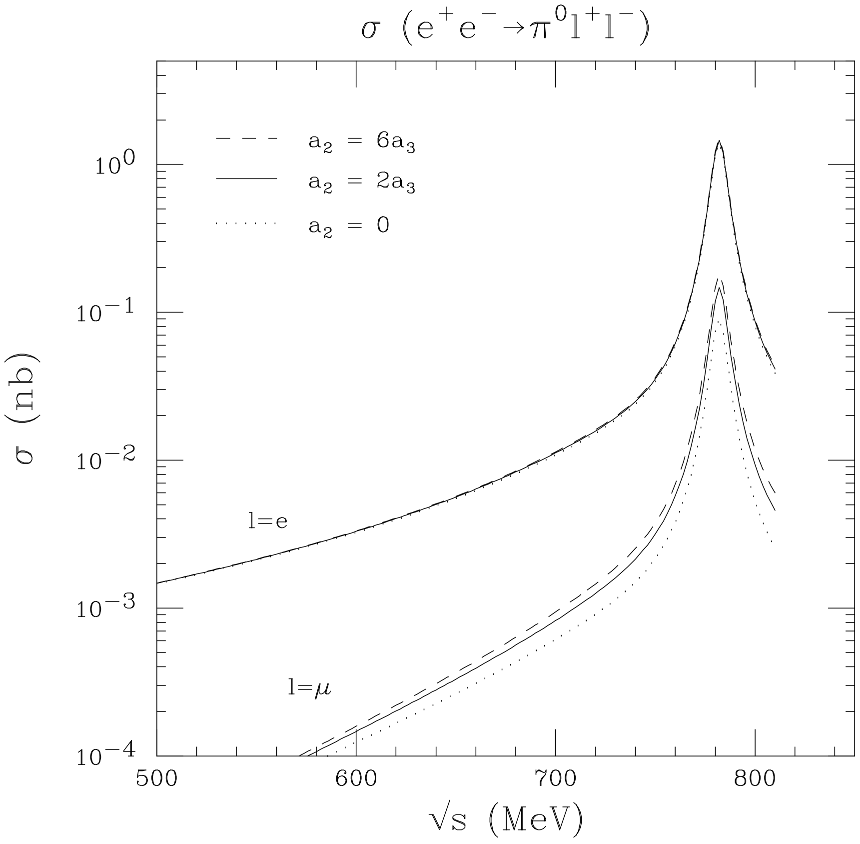

Figure 6: Cross-section for $e^+e^- \to \pi^0\mu^+\mu^-$ and $\pi^0e^+e^-$ for the quoted values of a_2 and a_3. VMD (solid line) requires $a_2 = 2a_3$. The dashed line corresponds to the alternative model with $a_2 = 6a_3$.

5.1 VMD Contribution

In conventional VMD models, the amplitude for the process $V^0 \to P^0P^0\gamma$ is obtained by calculating the Feynman diagrams shown in Fig.(7). All the couplings of our amplitudes can be deduced from the two previously presented lagrangians, eqs. (36,71), with $a_2 = -3/16\pi^2$. In addition to the $V\gamma$ couplings (38), which satisfactorily describe the set of data for $V \to P\gamma$, for processes like $\phi \to P^0\pi^0\gamma$, where $P = \pi^0$ or η, one needs to introduce a small contamination ϵ' of non-strange quarks in the ϕ meson. The relative amount can be deduced from the experimental [13] decay width $\Gamma(\phi \to \pi^0\gamma)$=5.8±0.6 KeV, which can be reproduced by VMD with

$$\epsilon' = 0.059 \pm 0.004, \qquad (49)$$

where the sign comes from observed $\omega - \phi$ interference effects in $e^+e^- \to \pi^+\pi^-\pi^0$ [13].

With our lagrangians and the quoted values for the coupling constants, let us now

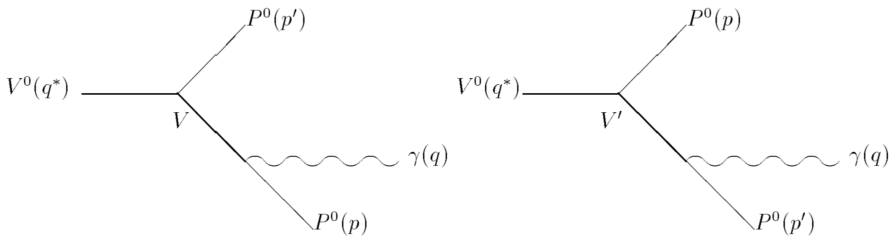

Figure 7: Feynman diagrams for the process $V^0 \to P^0 P^0 \gamma$ from Vector Meson contributions

turn to predict the intermediate vector-meson contributions to $V^0 \to P^0 P^0 \gamma$. ¿From the kinematical point of view these processes involve the two following amplitudes

$$\begin{aligned} \{a\} &= (\epsilon^* \cdot \epsilon)\ (q^* \cdot q) - (\epsilon^* \cdot q)\ (\epsilon \cdot q^*) \\ \{b(P)\} &= -(\epsilon^* \cdot \epsilon)\ (q^* \cdot P)\ (q \cdot P) - (\epsilon^* \cdot P)\ (\epsilon \cdot P)\ (q^* \cdot q) \\ &\quad +(\epsilon^* \cdot q)\ (\epsilon \cdot P)\ (q^* \cdot P) + (\epsilon \cdot q^*)\ (\epsilon^* \cdot P)\ (q \cdot P) \end{aligned} \tag{50}$$

where $\epsilon(\epsilon^*)$ are the polarizations of the final photon (initial vector meson), and q ($q^* = q + p + p'$) are the corresponding four-momenta; $P = p + q$, $P' = p' + q$ are those for the virtual (intermediate) vector mesons (V and V') of the direct and crossed terms (see Fig.(7)). The total VMD amplitude is then found to be

$$A(V^0 \to P^0 P^0 \gamma) = C(V^0 P^0 P^0 \gamma) \frac{G^2 e}{g\sqrt{2}} \left\{ \frac{P^2\{a\} + \{b(P)\}}{M_V^2 - P^2 - iM_V\Gamma_V} + \frac{P'^2\{a\} + \{b(P')\}}{M_{V'}^2 - P'^2 - iM_{V'}\Gamma_{V'}} \right\} \tag{51}$$

where $G = 3\sqrt{2}g^2/(4\pi^2 f)$ is the $\rho^0\omega\pi^0$ coupling constant and V^0 is the decaying vector meson. The intermediate ones, V and V', can be either the ω or the ρ-mesons, with $V = V'$ in $\pi^0\pi^0\gamma$ and $V \neq V'$ in $\eta\pi^0\gamma$-decays; for $\phi \to K^0 \bar{K}^0 \gamma$ one obviously has $V = K^{*0}$ and $V' = \bar{K^*}^0$. The coefficient C is the same for both terms (using SU(3)-symmetric couplings) and changes from process to process according to well-known quark-model or nonet-symmetry rules:

$$1 = C(\rho^0\pi^0\pi^0\gamma) = 3C(\omega\pi^0\pi^0\gamma) = \frac{3\sqrt{3}}{\sqrt{2}}C(\rho^0\pi^0\eta\gamma) = \sqrt{\frac{3}{2}}C(\omega\pi^0\eta\gamma) = -\frac{3}{\sqrt{2}}C(\phi K^0\bar{K}^0\gamma) \tag{52}$$

and

$$\epsilon' = 3C(\phi\pi^0\pi^0\gamma) = \sqrt{\frac{3}{2}}C(\phi\pi^0\eta\gamma) \tag{53}$$

for the ϕ-decays where the Zweig-rule is operative.

¿From the above amplitudes, the partial widths are obtained performing a numerical integration of

$$\Gamma(V \to PP'\gamma) = \left(\frac{1}{2}\right) \frac{1}{192\pi^3 M_V} \int dE_\gamma \int dE_P \sum_{pol} |A(V \to PP'\gamma)|^2 \tag{54}$$

where the factor (1/2) has to be included only for $\pi^0\pi^0$ decays.

Our results using the full VMD amplitudes (51) and the three-body phase space formulae (54) are shown in the two last columns of Table 1. For comparison we also include (first column) the upper limit for the three experimentally studied decay rates [13, 20] and the predictions of other authors [22, 23, 24] who have worked in our same context. Our results are not incompatible with those by Singer [25], who first noticed the simple relation $\Gamma(V^0 \to \pi^+\pi^-\gamma) = 2\Gamma(V^0 \to \pi^0\pi^0\gamma)$ for the VMD part of the rate. This relation allows for a comparison of our results with those by Renard [23], quoted (in parenthesis) in the second column of Table 1. The accompanying values are the original ones [23] corrected by the present-day data for $\Gamma(\omega \to \pi^0\gamma)$ and ϵ', and turn out to be in excellent agreement with our predictions. The agreement with ref.[24] is somewhat less satisfactory. Finally, we disagree in the complete list of numerical predictions quoted in ref.[22] even if the initial expressions for the lagrangians are the same, since that our coupling constant g has been defined as 1/2 of that in ref.[22].

Notice that the branching ratios (BR) appearing in the last column of Table 1, do not always coincide with the simple product of branching ratios for the individual vector dominated diagrams of Fig.(7). This point has been discussed in detail in ref.[26]

Concentrating on ϕ-decays one first observes that our vector-meson dominated mechanism predicts a completely negligible $\Gamma(\phi \to K^0\bar{K}^0\gamma)$, contrasting with the four orders of magnitude larger prediction from ref.[22]. We have carefully analyzed our calculation and, for this channel containing exclusively soft photons ($E \lesssim 25$ MeV), an analytic expression for the amplitude in this low-E limit has been obtained. One has

$$A(\phi \to K^0\bar{K}^0\gamma) \simeq \frac{eG^2}{3g(M_{K^*}^2 - m_{K^0}^2 - iM_{K^*}\Gamma_{K^*})}\Big[(p\cdot p' - m_{K^0}^2)\{a\} + \\ \epsilon^*\cdot(p-p')\ [(\epsilon\cdot p)\ (q\cdot p') - (\epsilon\cdot p')\ (q\cdot p)]\Big] \tag{55}$$

Table 1: Global contribution of intermediate vector mesons to decay rates (in eV) and branching ratios (last column) for different $V^0 \to P^0 P^0 \gamma$ transitions as predicted by several authors. Experimental upper limits are also quoted.

Decay rates (in eV)	EXP [13, 20]	Ref. [23]	Ref. [24]	Ref. [22]	This calculation	
					Γ	B.R.
$\Gamma(\rho \to \pi^0\pi^0\gamma)$	—	$(2.5)1.6 \cdot 10^3$	—	$4.3 \cdot 10^3$	$1.6 \cdot 10^3$	$1.1 \cdot 10^{-5}$
$\Gamma(\rho \to \pi^0\eta\gamma)$	—	—	—	593	0.061	$4 \cdot 10^{-10}$
$\Gamma(\omega \to \pi^0\pi^0\gamma)$	$< 3.4 \cdot 10^3$	(350) 227	—	690	235	$2.8 \cdot 10^{-5}$
$\Gamma(\omega \to \pi^0\eta\gamma)$	—	—	—	53	1.39	$1.6 \cdot 10^{-7}$
$\Gamma(\phi \to \pi^0\pi^0\gamma)$	$< 4.4 \cdot 10^3$	(250) 54	45	153	51	$1.2 \cdot 10^{-5}$
$\Gamma(\phi \to \pi^0\eta\gamma)$	$< 11 \cdot 10^3$	—	35	228	23.9	$5.4 \cdot 10^{-6}$
$\Gamma(\phi \to K^0\bar{K}^0\gamma)$	—	—	—	0.18	$1.2 \cdot 10^{-5}$	$2.7 \cdot 10^{-12}$

where p, p' are the pseudoscalar four-momenta, and

$$\sum |A(\phi \to K^0\bar{K}^0\gamma)|^2 = \frac{e^2G^4}{9g^2} \frac{(p \cdot p' - m_{K^0}^2)}{(M_{K^*}^2 - m_{K^0}^2)^2 + M_{K^*}^2\Gamma_{K^*}^2} \cdot \left[2(p \cdot p')\,(q^* \cdot q)^2 - (p \cdot p' + m_{K^0}^2)\,4(q \cdot p)\,(q \cdot p')\right] \tag{56}$$

accidentally containing the small numerical factor $(p \cdot p' - m_{K^0}^2) = (M_\phi^2 - 4m_{K^0}^2)/2$ [13]. In other words, the $\phi \to K^0\bar{K}^0\gamma$ decay is predicted to be exceptionally suppressed not only by the obviously scarce available phase-space but also due to an almost complete destructive interference in the amplitude, as explicitly shown in Fig.(8). (Reversing the sign of the interference term would enlarge the width by 2 orders of magnitude).

Our mechanism also predicts sizable contributions to $\phi \to \pi^0\pi^0\gamma$ and $\eta\pi^0\gamma$ decays. The corresponding photonic spectra are shown in Figs.(9) and (10), where the interference effects have again been separated.

These interference effects contribute to enhance the peak at high E in the $\phi \to \pi^0\pi^0\gamma$ spectrum. Roughly one-half of this decay contains a photon with an energy E in the narrow range 400 MeV $\lesssim E \lesssim 470$ MeV. Alternative mechanisms, such as $\phi \to f_0, a_0\gamma$ are expected to produce exclusively lower energy photons, thus minimizing the interferences and allowing for separated analyses, particularly in $\phi \to \pi^0\pi^0\gamma$. We also notice that our predictions for this (and $\phi \to \pi^0\eta\gamma$) decay include events with the $\pi^0\gamma$ and $\eta\gamma$ invariant mass on the ρ-peak. As discussed in [26] for the case of $\phi \to \pi^+\pi^-\pi^0$, our calculation implicitly contains simpler estimates in terms of two-body branching ratios. The latter imply [13] $BR(\phi \to \pi^0\pi^0\gamma) = \frac{1}{3}BR(\phi \to \rho\pi)BR(\rho \to \pi\gamma) \simeq 34 \times 10^{-6}$ and $BR(\phi \to \pi^0\eta\gamma) = \frac{1}{3}BR(\phi \to \rho\pi)BR(\rho \to \eta\gamma) \simeq 16.4 \times 10^{-6}$, only in marginal agreement

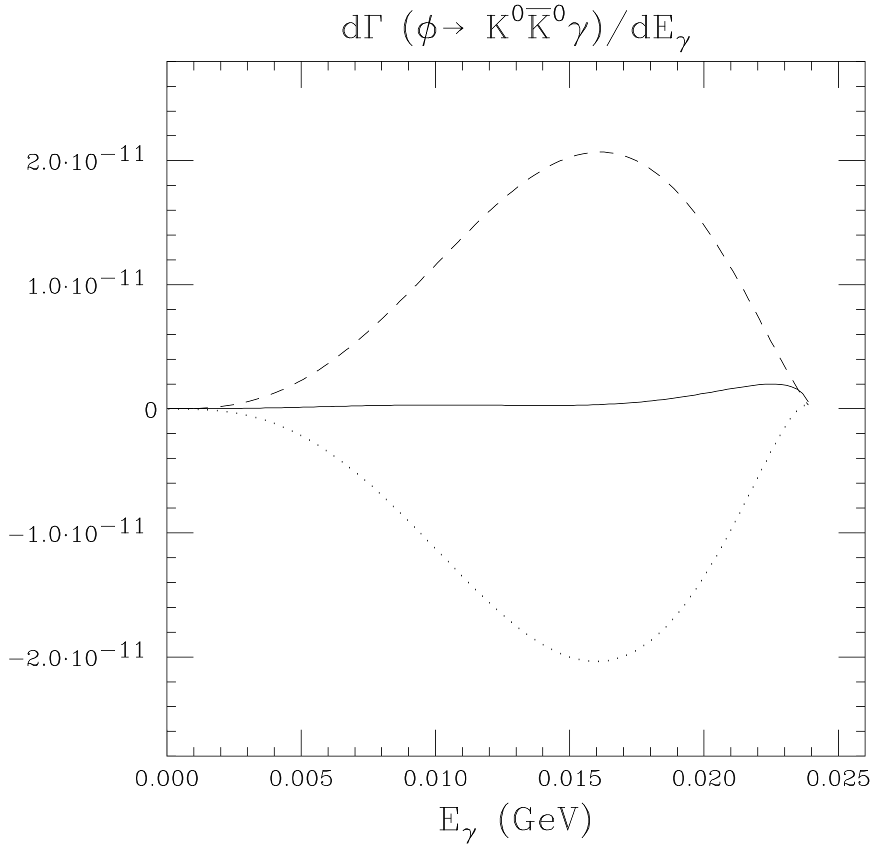

Figure 8: Photonic spectrum generated by intermediate vector-mesons in $\phi \to K^0\bar{K}^0\gamma$ (solid line). Dashed and dotted lines correspond to twice the contribution of a single diagram and their interference, respectively.

with our tabulated results because important interference and off-mass-shell effects have been neglected. We believe that our calculation should be prefered to these simpler estimate. However, these rough estimates are useful and allow for a numerical check of our predictions. Indeed, by artificially reducing the ρ-width in our complete (three-body) calculation one recovers the expected agreement with the above simpler (two-body) estimates discussed at the end of section 3 of [26].

5.2 Adding Chiral Loops

Let us now turn to the discussion of chiral loop contributions to the above processes. As mentioned, although strong, electromagnetic and weak interactions of pseudoscalar mesons P at low energies are known to be well described by effective chiral lagrangians, implementing the strict ChPT lagrangian with the effects of meson-resonances leads to a

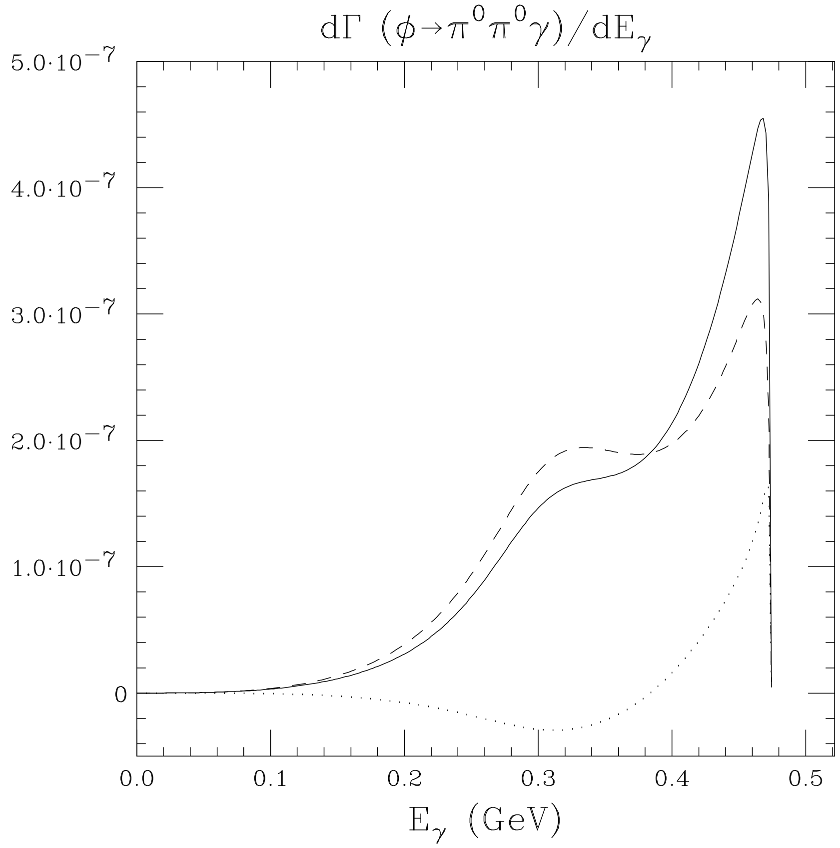

Figure 9: Photonic spectrum in $\phi \to \pi^0\pi^0\gamma$ with conventions as in Fig.(8).

more complete and realistic scheme with a largely increased predictive power. In particular, it can incorporate and improve most of the VMD results so far discussed.

For concreteness, let us consider $\phi \to \pi^0\pi^0\gamma$ decay for which a rather low branching ratio should be expected (see Table 1). There is a two-fold reason for that: neutral particles cannot radiate copiously (bremsstrahlung) photons and, moreover, the Zweig rule suppress ϕ-decays into pions. In the ChPT context this double suppression is at once avoided through the contributions of charged-kaon loops. If so, the smallness of the $\phi \to \pi^0\pi^0\gamma$ branching ratio will no longer hold and the analysis of this and related decays could evidentiate the effects of the (otherwise elusive) chiral loops. Notice, however, that we are pushing ChPT somewhat outside its original context which did not allow for the inclusion of ϕ and other resonances. Our purpose is to compute some consequences of this extended version of ChPT to allow for future comparison with experimental data.

Using the SU(3)-extended terms of the lagrangians (17),(18) or (23)

$$\mathcal{L}_{VPP} = ig\ tr(V_\mu\ P\ \partial^\mu P - V_\mu\ \partial^\mu P\ P) \tag{57}$$

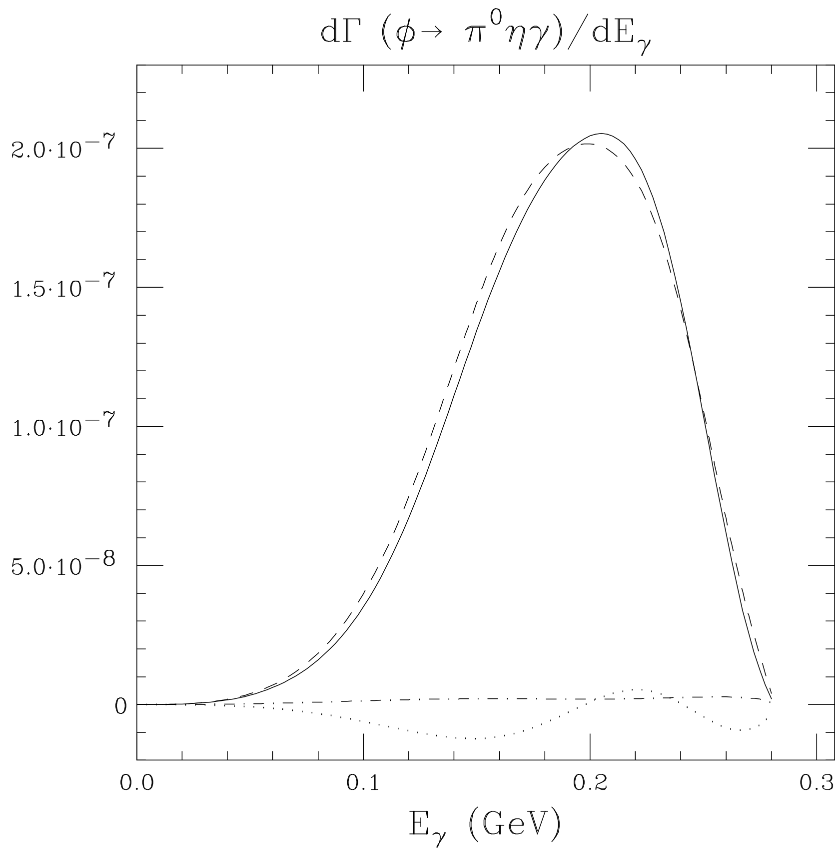

Figure 10: Photonic spectrum in $\phi \to \pi^0\eta\gamma$. Dashed and dot-dashed lines are the contributions of each diagram and the dotted line corresponds to their interference.

$$\mathcal{L}_{V\gamma} = -2egf^2 A^\mu \; tr(QV_\mu) \tag{58}$$

with $\sqrt{2}gf = M_V$, the V-meson mass, or $g \simeq 4.2$, we now calculate the ChPT-amplitudes for the decay processes $V^0 \to P^0P^0\gamma$. There is no tree-level contribution and at the one-loop level one requires computing the set of diagrams shown in Fig. (11). This leads to the amplitudes listed in sec.5 of ref.[26] and thus to the numerical contributions to the decay processes reported in Table 2.

Since VMD amplitudes can be interpreted as saturating the ChPT counterterms, the above mentioned contributions have to be added to obtain the whole ChPT amplitude. The relative weight of the two contributions so far discussed –the finite chiral loops versus the VMD amplitudes (51)– depends crucially on the decay mode. Let us first discuss $\rho^0 \to \pi^0\pi^0\gamma$ whose VMD contribution is given by eqs.(51) and (50) with the ω mass and width in both propagators. One easily obtains[21]

$$\Gamma(\rho^0 \to \pi^0\pi^0\gamma)_{VMD} = 1.62 \times 10^3 eV \tag{59}$$

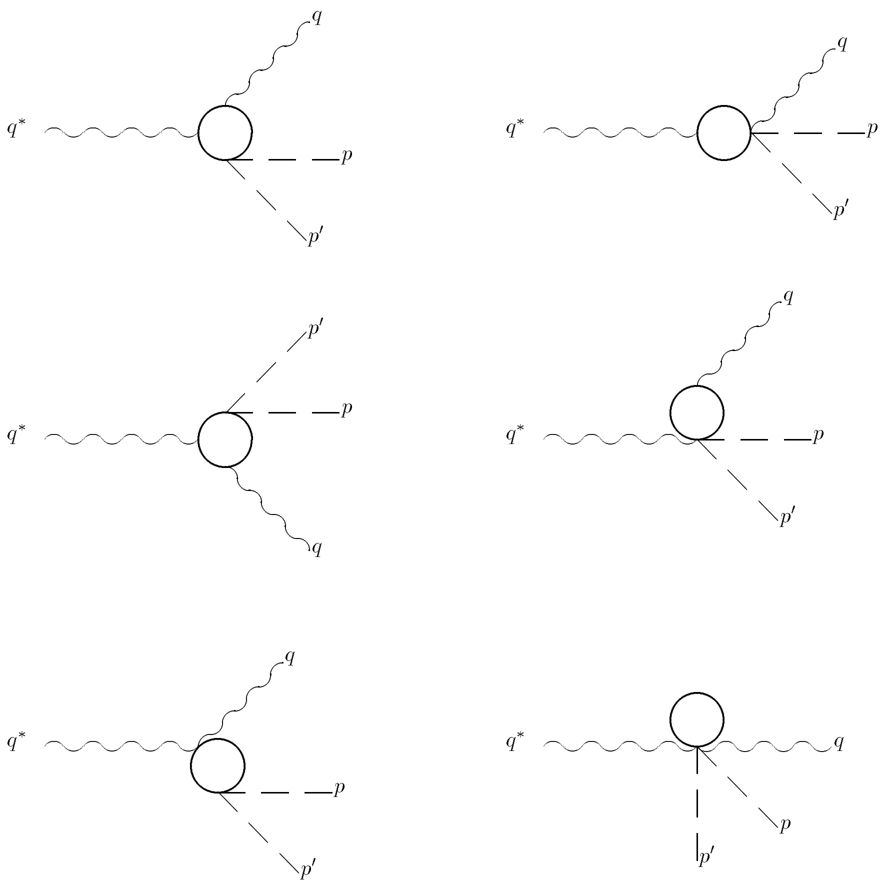

Figure 11: One loop diagrams for $V^0 \to P^0 P^0 \gamma$ decays. Charged-kaons or pions circulate along the loop

Table 2: Contribution of Chiral loops and intermediate vector mesons to decay rates (in eV) and branching ratios (last column) for different $V^0 \to P^0 P^0 \gamma$ transitions .

Decay rates (in eV)	Ch-loops	VMD	Total	B.R.
$\Gamma(\rho \to \pi^0\pi^0\gamma)$	1.42×10^3	1.62×10^3	3.88×10^3	26×10^{-6}
$\Gamma(\rho \to \pi^0\eta\gamma)$	0.006	0.061	$\simeq$VMD	VMD
$\Gamma(\omega \to \pi^0\pi^0\gamma)$	1.8	235	$\simeq$VMD	VMD
$\Gamma(\omega \to \pi^0\eta\gamma)$	0.013	1.39	$\simeq$ VMD	VMD
$\Gamma(\phi \to \pi^0\pi^0\gamma)$	224	51	269	61×10^{-6}
$\Gamma(\phi \to \pi^0\eta\gamma)$	131	23.9	157.5	36×10^{-6}
$\Gamma(\phi \to K^0\bar{K}^0\gamma)$	0.033	1.2×10^{-5}	$\simeq$ Ch- loops	7.6×10^{-9}

which is of the same order of magnitude as the pion-loop contribution [26], *i.e.*

$$\Gamma(\rho^0 \to \pi^0\pi^0\gamma)_\pi = 1.42 \times 10^3 eV. \tag{60}$$

The global $\rho^0 \to \pi^0\pi^0\gamma$ decay width is therefore given by the sum of the two amplitudes leading separately to eqs.(60) and (59). One obtains

$$\begin{aligned} \Gamma(\rho^0 \to \pi^0\pi^0\gamma) &= 3.88 \times 10^3 eV \\ BR(\rho^0 \to \pi^0\pi^0\gamma) &= 26 \times 10^{-6} \end{aligned} \tag{61}$$

and the photonic spectrum shown (solid line) in Fig.(12) clearly peaked at higher energies E_γ. The separated contributions from pion-loops and from VMD, as well as their interference, are also shown in Fig.(12) (dashed, dotdashed and dotted lines, respectively).

The situation changes quite clearly when turning to the other decay modes like ρ, $\omega \to \pi^0\eta\gamma$ and $\omega \to \pi^0\pi^0\gamma$. We find that the kaon-loop contributions are one or two orders of magnitude smaller [26],

$$\begin{aligned} \Gamma(\rho^0 \to \pi^0\eta\gamma)_K &= 0.006\ eV \\ \Gamma(\omega \to \pi^0\eta\gamma)_K &= 0.013\ eV\ , \quad \Gamma(\omega \to \pi^0\pi^0\gamma)_K = 1.8\ eV. \end{aligned} \tag{62}$$

The physical reason for this suppression is that the usually dominant pion-loops are isospin-forbidden in these decays. More accurate estimates and the shape of the photonic spectra seem unnecessary due to the smallness of the corresponding branching ratios (only the third one, $BR(\omega \to \pi^0\pi^0\gamma) \simeq 28 \times 10^{-6}$, could reasonably allow for detection) and also to the fact that these decay modes are dominated by the well-understood (see [21]) but less-interesting VMD contribution.

By contrast the latter VMD-contribution is expected to be much smaller in $\phi \to \pi^0\eta\gamma$ and $\pi^0\pi^0\gamma$ decays due to the Zweig rule, as shown in Table 1, well below the kaon-loop

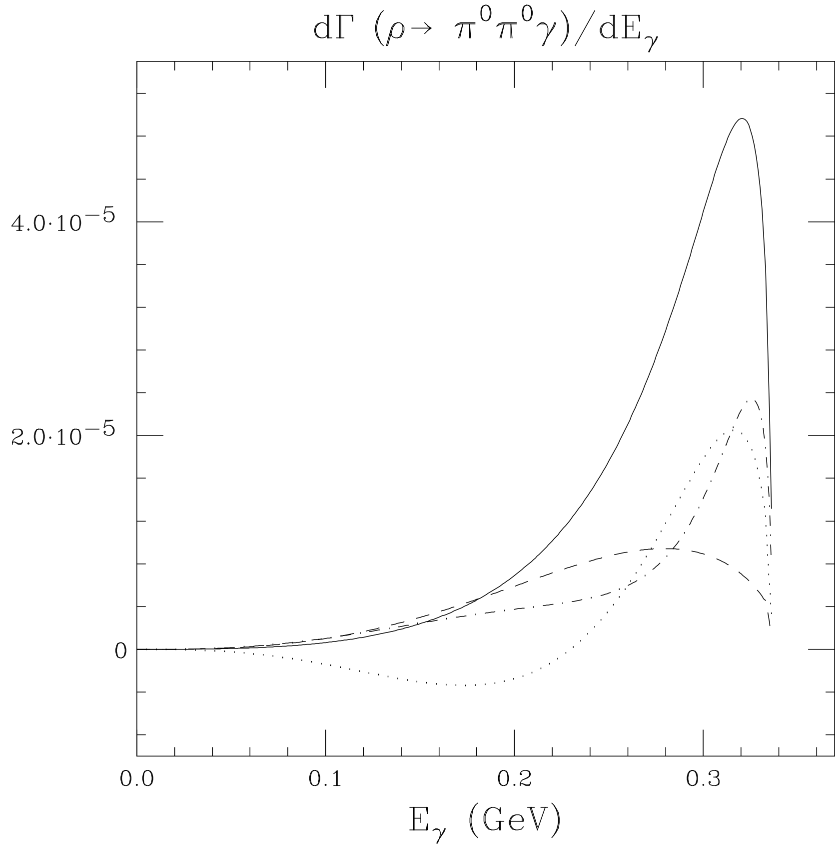

Figure 12: Photonic spectrum in $\rho^0 \to \pi^0\pi^0\gamma$ (solid line). Dashed line corresponds to the contribution of pion-loops, dotdashed line is the VMD contribution, and dotted line is their interference.

contributions, $\Gamma(\phi \to \pi^0\eta\gamma)_K = 131\ eV$ and $\Gamma(\phi \to \pi^0\pi^0\gamma)_K = 224\ eV$. Proceeding as before and adding the corresponding amplitudes with the appropriate phases leads to

$$\begin{aligned} \Gamma(\phi \to \pi^0\eta\gamma) &= 157.5\ eV \qquad \Gamma(\phi \to \pi^0\pi^0\gamma) = 269\ eV \\ BR(\phi \to \pi^0\eta\gamma) &= 36 \times 10^{-6} \qquad BR(\phi \to \pi^0\pi^0\gamma) = 61 \times 10^{-6} \end{aligned} \tag{63}$$

and the photonic spectra shown in Fig.(13) and (14).

The Zweig allowed kaon-loops are seen to dominate both spectra and decay rates of the above ϕ-decays and the predicted branching ratios are large enough to allow for detection and analyses in future ϕ-factories. For completeness we have also computed $\Gamma(\phi \to K^0\bar{K}^0\gamma) \simeq \Gamma(\phi \to K^0\bar{K}^0\gamma)_K \simeq 0.033$ eV, with $BR(\phi \to K^0\bar{K}^0\gamma) \simeq 7.6 \times 10^{-9}$, again dominated by kaon-loops (due to the smallness of the VMD contribution discussed in detail before and in ref. [21]). Notice that our computation does not include scalar meson contributions, wich are expected to be of the same order of magnitude [27, 28, 29].

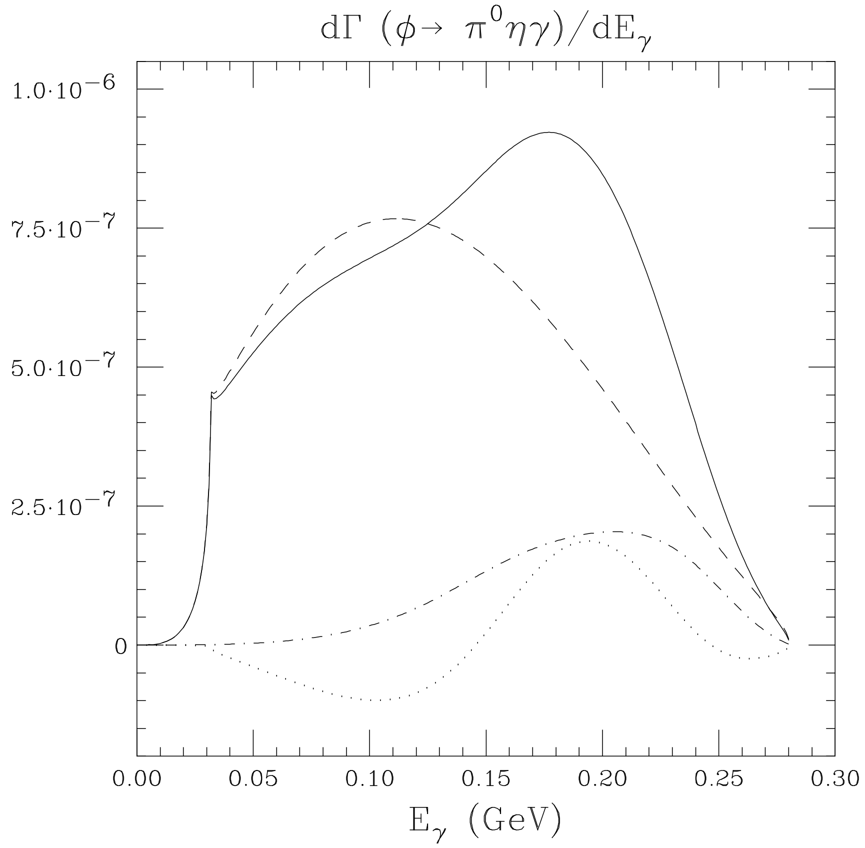

Figure 13: Photonic spectrum in $\phi \to \pi^0\eta\gamma$ (solid line). Dashed line corresponds to the contribution of kaon loops, dotdashed line is the VMD contribution, and dotted line is their interference.

Our results represent therefore a well defined background to these latter, more interesting contributions.

In summary, the well understood contributions of intermediate vector mesons in $V^0 \to P^0P^0\gamma$ decays have been discussed. Vector Meson Dominance alone predicts $BR(\phi \to \pi^0\pi^0\gamma) = 12 \times 10^{-6}$ and $BR(\phi \to \pi^0\eta\gamma) = 5.4 \times 10^{-6}$, and a characteristic photonic spectrum (peaked at higher energies) in the first decay. Similarly, an exceptionally small contribution is predicted (and its physical origin understood) for the branching ratio $BR(\phi \to K^0\bar{K}^0\gamma)$, namely, $\sim 2.7 \times 10^{-12}$. Other VMD predictions are $BR(\omega \to \pi^0\pi^0\gamma) \simeq 28 \times 10^{-6}$ and $BR(\rho^0 \to \pi^0\pi^0\gamma) \simeq 11 \times 10^{-6}$.

On the other hand, we find that some vector meson decays into two neutral pseudoscalars and a photon could receive important contributions from chiral loops if ChPT is extended in the plausible and well defined way proposed here. Some consequences of this extension –the relevance of pion-loops in $\rho \to \pi^0\pi^0\gamma$ and the dominance of kaon-loops in

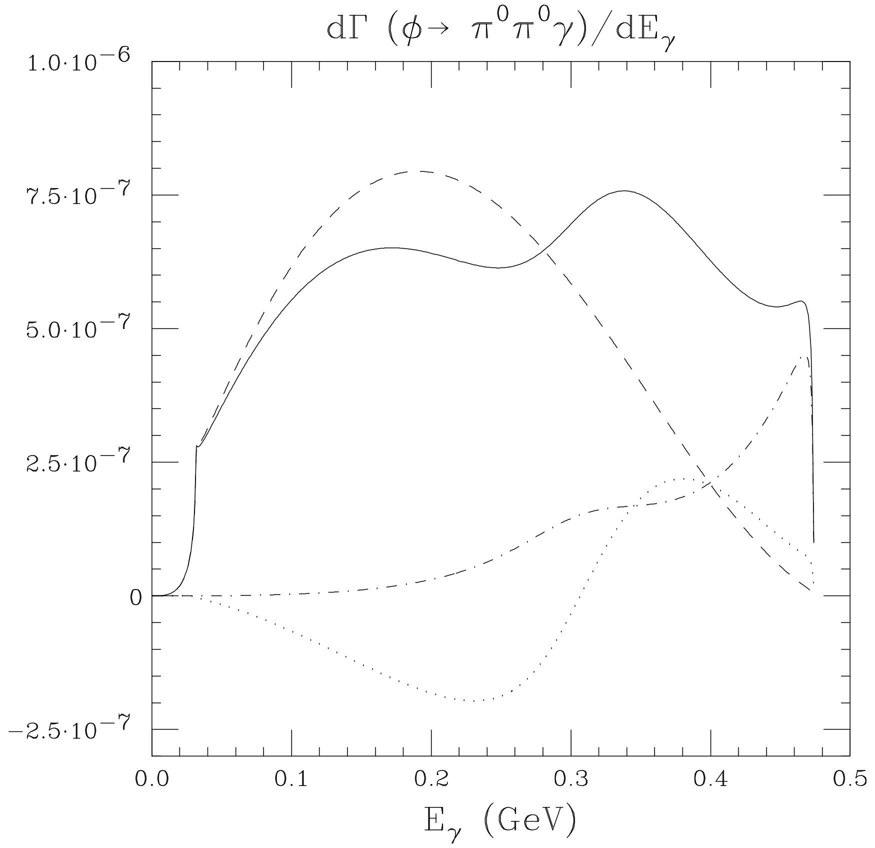

Figure 14: Photonic spectrum in $\phi \to \pi^0\pi^0\gamma$ with conventions as in Fig.(13).

$\phi \to \pi^0\eta\gamma$, $\pi^0\pi^0\gamma$– have been unambigously predicted thus allowing for future comparison with data. If the latter turn out to confirm our predictions the domain of applicability of ChPT and their relevance would be considerably increased.

6 SU(3)-breaking effects in the non-anomalous sector

Our purpose in this section and the one to follow consists in attempting to go one step beyond the successful description of the low-energy interactions of the pseudoscalar-meson octet. This is done by refining the predictions of the above schemes through the introduction of a well-known effect in hadron physics, namely, SU(3)-breaking in the vector-meson sector, a refinement that forthcoming data will certainly require.

With the "hidden symmetry" lagrangian discussed in sect. 2, one can attempt the description of the following sets of data (that we take from [13] neglecting error bars):

- the vector meson mass spectrum

$$M^2_{\rho,\omega},\ M^2_{K^*},\ M^2_{\phi} = 0.60,\ 0.80,\ 1.04\ GeV^2; \tag{64}$$

- the weak decay constants

$$f_\pi = 132\ MeV, \quad f_K = 160\ MeV; \tag{65}$$

- the $\rho-\gamma, \omega-\gamma$ and $\phi-\gamma$ conversion factors, $f_{V\gamma} \equiv \dfrac{eM_V^2}{f_V}$ (see eq.(38)), extracted from $\Gamma(V \to e^+e^-)$

$$f_{\rho\gamma},\ f_{\omega\gamma},\ f_{\phi\gamma} = (\ 36,\ 11,\ -26\ ) \times 10^{-3}\ GeV^2 \tag{66}$$

- the vector meson decay constants $g_{\rho\pi\pi} = \sqrt{2}\ g$, $g_{K^*K\pi} = \sqrt{3}\ g/\sqrt{2}\ g_{\phi KK} = \sqrt{2}\ g$ obtained from $\Gamma(V \to PP)$

$$g_{\rho\pi\pi} = 6.1,\ g_{K^*K\pi} = 5.5,\ g_{\phi KK} = 6.5 \tag{67}$$

¿From [30] we take the following experimental values for the electromagnetic (e.m.) charge radii

$$\begin{aligned} < r^2_{\pi^+} > &= 0.44 \pm 0.03\ fm^2 \\ < r^2_{K^+} > &= 0.31 \pm 0.05\ fm^2 \\ - < r^2_{K^0} > &= 0.054 \pm 0.026\ fm^2 \end{aligned} \tag{68}$$

and the combined result, free from most systematic errors (see Dally et al. and Amendolia et al. in ref.[30])

$$< r^2_{\pi^+} > - < r^2_{K^+} > = 0.13 \pm 0.04\ fm^2 \tag{69}$$

The most immediate possibility to account for the above sets of data consists in using the "hidden symmetry lagrangian" (19) as a self contained effective theory in the good SU(3) limit. In this case, the SU(3)-breaking effects shown by some of the above data remain unexplained but two successful relations can be obtained for the non-strange sector. The lagrangian (19) predicts $M^2_{\rho,\omega} = 2g^2f^2$ in the $0.50 - 0.60\ GeV^2$ range when the values (65) for f are used together with the range of values for g obtained from $f_{V\gamma}$ (66) and g_{VPP}(67). This agrees with the value coming from the direct measurement of the ρ, ω mass (64). Moreover, it also agrees with that coming from the pion charge radius, leading in our approach to $M^2_\rho = 6/ < r^2_\pi > = 0.51\ GeV^2$. Alternatively, in a ChPT context, one can use lagrangian (19) to saturate the finite part of the required counterterms and then include the chiral-logs from the loop corrections. One obtains [31] (apart from the successful relation $M^2_{\rho,\omega} = 2g^2f^2$, as before) a vanishing value for the SU(3)-breaking low-energy counterterm L_5, eq.(6), and $L_9 = f^2/4M^2_\rho$, eq. (5). With this latter value in

(8) and evaluating the chiral-log correction at the conventional value $\mu = M_\rho$, one predicts $< r_\pi^2 > = 0.46\ fm^2$ in very good agreement with the experimental data (68).

Including SU(3)-breaking effects, one can further improve this situation [31]. Since the pseudoscalar sector is known to break the symmetry as in eq.(4), *i.e.*, proportionally to $Tr(\xi_R M \xi_L^\dagger + \xi_L M \xi_R^\dagger)$, we incorporate SU(3) symmetry breaking, as already attempted in ref.[2], via a similar hermitian combination $(\xi_L \epsilon \xi_R^\dagger + \xi_R \epsilon \xi_L^\dagger)$ in both $\mathcal{L}_A$ and $\mathcal{L}_V$ terms, i.e.,

$$\mathcal{L}_A + \Delta\mathcal{L}_A = \frac{-f^2}{8} Tr\left\{ \left(D_\mu \xi_L \cdot \xi_L^\dagger - D_\mu \xi_R \cdot \xi_R^\dagger \right)^2 \left[1 + \left(\xi_L \epsilon_A \xi_R^\dagger + \xi_R \epsilon_A \xi_L^\dagger \right) \right] \right\} \tag{70}$$

and

$$\mathcal{L}_V + \Delta\mathcal{L}_V = \frac{-f^2}{8} Tr\left\{ \left(D_\mu \xi_L \cdot \xi_L^\dagger + D_\mu \xi_R \cdot \xi_R^\dagger \right)^2 \left[1 + \left(\xi_L \epsilon_V \xi_R^\dagger + \xi_R \epsilon_V \xi_L^\dagger \right) \right] \right\} \tag{71}$$

The matrix $\epsilon_{A(V)}$ is taken to be $\epsilon_{A(V)} = diag(0, 0, c_{A(V)})$, where $c_{A,V}$ are the SU(3) -breaking real parameters to be determined. Notice that the SU(3)-breaking terms, $\Delta\mathcal{L}_{A,V}$, are hermitian, thus differing from those in ref.[2]. Fixing the unitary gauge $\xi_L^\dagger = \xi_R = \xi = exp(iP/f)$, $(\sigma = 0)$, and expanding in terms of the pseudoscalar fields, one observes that the kinetic terms in $\mathcal{L}_A$ have to be renormalized. This is simply achieved rescaling the pseudoscalar fields [2]

$$\sqrt{1 + c_A}\ K \to K, \quad \sqrt{1 + 2c_A/3}\ \eta \to \eta \tag{72}$$

where an η-η' mixing angle of -19.5^0 has been used for the η case.

The physical content of this new, SU(3)-broken "hidden symmetry" lagrangian (70) and (71) can now be easily worked out. ¿From $a\,(\mathcal{L}_V + \Delta\mathcal{L}_V)$, we obtain the conventional SU(3)-splitting for the vector meson masses $(a = 2)$.

$$M_\rho^2 = M_\omega^2 = 2g^2 f^2, \qquad M_{K^*}^2 = M_\rho^2 (1 + c_V), \qquad M_\phi^2 = M_\rho^2 (1 + 2c_V) \tag{73}$$

For the V-γ couplings, the corresponding part of the lagrangian is explicitly given by:

$$\begin{aligned} \mathcal{L}_{V\gamma} &= -egf^2 A_\mu\ Tr\left[\{Q, V^\mu\}\ (1 + 2\epsilon_V) \right] \\ &= -\frac{eM_{\rho,\omega}^2}{\sqrt{2}g}\ A_\mu \left[\rho^{0\mu} + \frac{\omega^\mu}{3} - (1 + 2c_V)\frac{\sqrt{2}}{3}\phi^\mu \right] \end{aligned} \tag{74}$$

The new terms in the lagrangian (70,71) also induce an SU(3) symmetry breaking in the g_{VPP} coupling constants. One obtains

$$\begin{aligned} g_{\rho\pi\pi} &= \sqrt{2}\ g \\ g_{\rho KK} &= g_{\omega KK} = \frac{g}{\sqrt{2}}\ \frac{1}{1 + c_A} \\ g_{\phi KK} &= \sqrt{2}\ g\ \frac{1 + 2c_V}{1 + c_A} \\ g_{K^* K\pi} &= \frac{\sqrt{3}}{\sqrt{2}}\ g\ \frac{(1 + c_V)}{\sqrt{1 + c_A}} \end{aligned} \tag{75}$$

where the c_A-dependence comes from the symmetry breaking in the $\mathcal{L}_A + \Delta\mathcal{L}_A$ lagrangian due to the renormalization of the pseudoscalar fields (see eq.(72)). This redefinition of the pseudoscalar fields also implies symmetry breaking of their decay constants, namely,

$$f_K = \sqrt{1 + c_A}\ f_\pi, \qquad f_\eta = \sqrt{1 + 2c_A/3}\ f_\pi \tag{76}$$

One can now attempt a description of the whole set of data (64-68) in terms of, solely, the SU(3)-broken lagrangian (70) and (71). This fixes the values of the two new free parameters to $c_V = 0.30$ and $c_A = 0.45$. The fit is quite satisfactory for the four sets of data quoted in eqs.(64) to (67). For the pseudoscalar charge radii, one gets from eqs.(74, 75, 76)

$$\begin{aligned}
< r^2_{\pi^+} > &= \frac{6}{M^2_\rho} \\
< r^2_{K^+} > &= \frac{< r^2_{\pi^+} >}{(1 + c_A)} \frac{1}{3} \left(2 + (1 + 2c_V) \frac{M^2_{\rho,\omega}}{M^2_\phi} \right) \\
- < r^2_{K^0} > &= \frac{< r^2_{\pi^+} >}{(1 + c_A)} \frac{1}{3} \left(1 - (1 + 2c_V) \frac{M^2_{\rho,\omega}}{M^2_\phi} \right)
\end{aligned} \tag{77}$$

and the above values of c_V and c_A imply

$$< r^2_{\pi^+} >= 0.39\ fm^2, \qquad < r^2_{K^+} >= 0.26\ fm^2, \qquad - < r^2_{K^0} >= 0.01\ fm^2 \tag{78}$$

somewhat below (one or two σ's) the experimental data (68).

As previously discussed, a more sophisticated possibility is to use our SU(3)-broken lagrangian (70,71) in conjunction with ChPT. This can only modify the predictions for f_P and $< r^2_P >$ related to processes without vector-mesons in the external legs. The chiral-logs in eq.(7), evaluated at the conventional value $\mu = M_\rho$, account now for some 35% of the observed difference between f_K and f_π, thus requiring a smaller contribution from the L_5 counterterm and, hence, a smaller value for c_A. Accordingly, the best global fit is now achieved by the slightly modified values

$$c_V = 0.28 \qquad c_A = 0.36 \tag{79}$$

which preserve the goodness of the preceding fit for M_V, $f_{V\gamma}$, g_{VPP} and f_P, while improving the agreement in the $< r^2_P >$ sector. Indeed, on the one hand, the chiral-logs in eq.(8) enhance the previous predictions for $< r^2_{\pi^+,K^+} >$ leading to

$$< r^2_{\pi^+} >= 0.46 fm^2, \qquad < r^2_{K^+} >= 0.32 fm^2 \tag{80}$$

in better agreement with the data (68). On the other hand, making more explicit SU(3) breaking effects, one also obtains

$$\begin{aligned}
- < r^2_{K^0} > &= \frac{1}{16\pi^2 f^2}\, ln \frac{m^2_K}{m^2_\pi} + \frac{2}{1 + c_A} \left[\frac{1}{M^2_\rho} - \frac{(1 + 2c_V)}{M^2_\phi} \right] = 0.043\ fm^2 \\
< r^2_{\pi^+} > - < r^2_{K^+} > &= \frac{1}{16\pi^2 f^2}\, ln \frac{m^2_K}{m^2_\pi} + \frac{6}{M^2_\rho} - \frac{2}{1 + c_A} \left[\frac{2}{M^2_\rho} + \frac{(1 + 2c_V)}{M^2_\phi} \right] = 0.14\ fm^2
\end{aligned} \tag{81}$$

Table 3: (all data are in fm^2)

	$exp.[30]$	$ChPT[3]$	$SU(3)broken$ HS	$SU(3)broken$ $HS+Ch.loops$
$< r^2_{\pi^+} >$	0.44 ± 0.03	0.44	0.39	0.46
$< r^2_{K^+} >$	0.31 ± 0.05	0.40	0.26	0.32
$- < r^2_{K^0} >$	0.054 ± 0.026	0.036	0.01	0.043
$< r^2_{\pi^+} > - < r^2_{K^+} >$	0.13 ± 0.04	0.036	0.13	0.14

which considerably improve the one-loop ChPT results [3] quoted in the last line of eq.(8), namely $- < r^2_{K^0} >=< r^2_{\pi^+} > - < r^2_{K^+} >= 0.036\ fm^2$, significantly below the datum (69). The reason for this improvement stems from the fact that saturating the ChPT counterterms with our SU(3)-broken lagrangian one goes beyond the fourth order counterterms in ChPT, such as the SU(3)-symmetric counterterm L_9, and introduces corrections from its SU(3)-breaking analogues belonging to sixth order counterterm(s) in $\mathcal{L}^{(6)}$. This is explicitly seen in eqs.(81), which reduce to the conventional ChPT result (8) only in the good SU(3) limit $c_A = c_V = 0$ and $M^2_{\rho,\omega} = M^2_\phi$. We summarize the above in Table 3, where we indicate the results obtained for the charged radii in the three models so far discussed, i.e. chiral perturbation theory (ChPT) and SU(3) broken "Hidden Symmetry" (HS) scheme with and without chiral loops.

One can easily extend the above results for the e.m. charge radii of pseudoscalars to include their weak analogue in K_{l3} decays. Sirlin's theorem [32], valid up to first order in SU(3)-breaking, and requiring

$$< r^2_{K\pi} > - < r^2_{K^0} >= \frac{1}{2} < r^2_{\pi^+} > + \frac{1}{2} < r^2_{K^+} > \tag{82}$$

provides the clue. The data (68) and the experimental value [13] $< r^2_{K\pi} >= 0.36 \pm 0.02\ fm^2$ are fully compatible with Sirlin's theorem (82) thus reinforcing the significance of our discussion on charge radii (recall that only one experiment has measured that for the neutral kaon). On the other hand, the predictions of our first-order SU(3)-breaking lagrangian verify (as they must) the theorem, thus checking our calculations and providing their authomatic extension to the $K\pi$ case. From the expression

$$< r^2_{K\pi} >= \frac{1 + c_V}{\sqrt{1 + c_A}} \frac{6}{M^2_{K^*}} + \ chiral\ loop\ contributions \tag{83}$$

where the contribution from chiral loops is the one to be found in ref. [3], we obtain the very acceptable value $< r^2_{K\pi} >= 0.33\ fm^2$. The above equation can be compared with the chiral perturbation theory result [3]

$$< r^2_{K\pi} >= \ chiral\ loop\ contributions\ + \frac{24}{f^2} L_9(\mu) \tag{84}$$

which gives $< r^2_{K\pi} >= 0.38\ fm^2$.

7 SU(3)-breaking effects in the anomalous (W-Z) sector

We shall now extend the above treatment to processes related to the anomaly or Wess-Zumino lagrangian. Notice that introducing our value $c_A = 0.36$, eq.(79), in eq.(76) for f_η, leads to $\Gamma(\eta \to \gamma\gamma) = 0.53$ KeV quite in line with the datum [13] $\Gamma(\eta \to \gamma\gamma) = 0.46 \pm 0.05$ KeV. This encourages to try a full treatment, similar to the one discussed so far, to the anomalous sector. Our purpose is to calculate the effects of SU(3) symmetry breaking in radiative decays of vector mesons, we have then to consider the part of the Lagrangian related to the WZ anomaly and we can expect, in analogy with what was done so far, that these effects will require the introduction of one more parameter in the discussion, which will be called c_{WZ} (see later). It will then be necessary to reconsider all the successfull numerical tests obtained so far and try to perform a single global fit to both the anomalous and non-anomalous sector with the three SU(3) breaking parameters c_A, c_V, c_{WZ}. We shall first proceed by obtaining relations between the relevant couplings in the anomalous sector and try to determine the parameters, independently of what was done before.

We start with vector–vector–pseudoscalar meson (VVP) interactions as contained in the SU(3)-symmetric VVP lagrangian introduced in ref. [2]. Inserting as before the additional, symmetry breaking term $(\xi_L \epsilon \xi_R^\dagger + \xi_R \epsilon \xi_L^\dagger)$ in an appropriate way to get an hermitian Lagrangian, the total broken Lagrangian can now be written as

$$\mathcal{L}_{VVP} + \Delta\mathcal{L}_{VVP} = \frac{G_P}{\sqrt{2}} \epsilon^{\mu\nu\rho\sigma} Tr\left[\partial_\mu V_\nu \left(1 + 2\epsilon_{WZ}\right) \partial_\rho V_\sigma P\right] \tag{85}$$

where $\epsilon_{WZ} = diag(0, 0, c_{WZ})$, c_{WZ} is the breaking parameter in the anomalous sector, and $G_P = 3\sqrt{2}g^2/4\pi^2 f_P$ is the strong VVP coupling constant, where the c_A-dependent f_P factor (see eq.(76)) already includes the part of the effects of SU(3) breaking coming from the renormalization of the pseudoscalars fields in the $\mathcal{L}_A$ lagrangian.

With this conventions, $G_\pi = 3\sqrt{2}g^2/4\pi^2 f_\pi$ is the $\rho^0\omega\pi^0$ coupling constant (see section 4) which contains no SU(3)-breaking and whose value can be obtained from the experimental radiative decay width [13] $\Gamma(\omega \to \pi^0\gamma) = 0.72 \pm 0.05$ MeV. G_π can also be obtained extracting a value for $g = 4.1 \pm 0.2$ from $\rho \to \pi\pi$ and $\rho, \omega \to e^+e^-$ decay data [13]. Using $f_\pi = 132$ MeV, we then obtain $\Gamma(\omega \to \pi^0\gamma) = 0.74$ MeV in good agreement with the experimental result. In our normalization, the radiative decay widths for vector mesons are given by

$$\Gamma(V \to P\gamma) = \frac{1}{3}\alpha\ g^2_{VP\gamma}\ q^3_\gamma, \qquad q_\gamma = \frac{M_V^2 - M_P^2}{2M_V} \qquad g_{VP\gamma} = \sum_{V'} \frac{g_{VV'P}\ g_{V'\gamma}}{M^2_{V'}} \tag{86}$$

where the relevant coupling constants take into account that these decays proceed via intermediate vector mesons V'. Thanks to this, one immediately recovers the successful relation (10), $F_{LO}^{ChPT} = g_{\pi\gamma\gamma} = \sqrt{2}\ \alpha/\pi\ f_\pi$, coming from the WZ anomaly and satisfied by the experimental $\pi^0 \to \gamma\gamma$ decay rate.

The coupling constants $g_{V\gamma}$ are easily obtained from the lagrangian in eq.(74) defined in the previous section. One then obtains

$$g_{\rho\gamma} = 3\ g_{\omega\gamma} = M^2_{\rho,\omega}/\sqrt{2}g \qquad g_{\phi\gamma} = -M^2_{\rho,\omega}(1+2c_V)/3g \tag{87}$$

which are the SU(3) broken modifications of the usual $V\gamma$ couplings with all equal masses (38). It is interesting to see how one can achieve both consistency with the unbroken case successful relations as well as with the experimental value of the V-masses, if one choose a value for the parameter c_V such that

$$M^2_\rho(1+2c_V) = M^2_\phi \tag{88}$$

This is achieved by choosing $c_V = 0.36$, not far from the range of values for which a good fit to a large number of other low energy constant was obtained in the previous section. With this choice, we then have $g_{\phi\gamma} = -M^2_\phi/3g$ and using eqs.(86), (87) and the broken VVP Lagrangian (85) to extract the $g_{VV'P}$ couplings, we obtain the following expressions for the coupling constants $g_{VP\gamma}$

$$\begin{aligned}
g_{\omega\pi^0\gamma} &= \frac{G_\pi}{\sqrt{2}g} & g_{\rho^0\pi^0\gamma} &= \frac{1}{3}g_{\omega\pi^0\gamma} \\
g_{\omega\eta\gamma} &= \frac{\sqrt{2}}{3\sqrt{3}}\frac{f_\pi}{f_\eta}(1-\sqrt{2}\epsilon')g_{\omega\pi^0\gamma} & g_{\rho\eta\gamma} &= \frac{\sqrt{2}}{\sqrt{3}}\frac{f_\pi}{f_\eta}g_{\omega\pi^0\gamma} \\
g_{\phi\eta\gamma} &= \frac{2}{3\sqrt{3}}\frac{f_\pi}{f_\eta}\left(1+2c_{WZ}+\frac{\epsilon'}{\sqrt{2}}\right)g_{\omega\pi^0\gamma} & g_{\phi\pi^0\gamma} &= \epsilon'\ g_{\omega\pi^0\gamma} \\
g_{K^{*0}K^0\gamma} &= -\frac{2}{3}\frac{f_\pi}{f_K}(1+c_{WZ})g_{\omega\pi^0\gamma} & g_{K^{*\pm}K^\pm\gamma} &= \frac{1}{3}\frac{f_\pi}{f_K}(1-2c_{WZ})g_{\omega\pi^0\gamma}
\end{aligned} \tag{89}$$

The parameter ϵ' is the one introduced in section 4, eq.(49), to account for the small contamination of non–strange (strange) quarks in the ϕ (ω) meson. Notice that, because of eq.(88), the parameter c_V disappears from the above relations, which now contain only c_A and c_{WZ}. The value of the anomalous breaking parameter c_{WZ} can be directly obtained from the ratio between the experimental decay widths [13] $K^{*0} \to K^0\gamma$ and $K^{*\pm} \to K^\pm\gamma$. The ratio depends only from c_{WZ} and leads immediately to $c_{WZ} = -0.10 \pm 0.03$, whereas for c_A we can use eq.(76) and the experimental results

$$\frac{f_K}{f_\pi} = 1.22 \pm 0.02, \quad \frac{f_\eta}{f_\pi} = 1.06 \pm 0.08 \tag{90}$$

which lead to the value $c_A = 0.45$ as obtained in the previous section.

At this point, the set of SU(3) breaking parameters c_V, c_A, c_{WZ} can be put to a test by calculating the V radiative decay widths following eq.(86) with the coupling constants

Table 4:

$Decay$	$\Gamma(keV)$	$\Gamma(keV)$	$\Gamma(keV)$
$V \to P\gamma$	$exp.$ $(ref.[13])$	$c_A = 0.44 \pm 0.04$ $c_{WZ} = -0.1 \pm 0.03$	$c_A = 0.36$ $c_V = 0.28$ $c_{WZ} = -0.05$
$\omega \to \pi^0\gamma$	716 ± 43	740 ± 70	740
$\rho \to \pi\gamma$	76 ± 10	67 ± 6	67
$\omega \to \eta\gamma$	4 ± 2	5.2 ± 0.6	5.4
$\rho \to \eta\gamma$	58 ± 11	47 ± 6	49
$\phi \to \eta\gamma$	56.7 ± 2.8	53 ± 8	55
$\phi \to \pi^0\gamma$	5.8 ± 0.6	5.7 ± 0.7	5.7
$K^{*0} \to K^0\gamma$	117 ± 10	101 ± 14	107
$K^{*\pm} \to K^{\pm}\gamma$	50 ± 5	44 ± 6	47

given by eq.(89). Our results, obtained using $g = 4.1 \pm 0.2$ and $\epsilon' = 0.058 \pm 0.004$, as well as $c_A = 0.44 \pm 0.04$ and $c_{WZ} = -0.10 \pm 0.03$ for the symmetry breaking parameters, are shown in Table 4. For comparison we also include the corresponding experimental decay widths as taken from ref.[13] (in the $\rho \to \pi\gamma$ case we have averaged for neutral and charged decays). The description of all these data turns out to be quite satisfactory, with SU(3)-breaking effects playing a central role in some cases. As already noted by Hajuj [33], a non-vanishing value for c_A (thus achieving $f_\pi < f_\eta < f_K$) is essential to reduce the predicted $\phi \to \eta\gamma$ and $K^{*0} \to K^0\gamma$ decay rates to their experimental values. Our value $c_{WZ} = -0.10 \pm 0.03$ is also crucial to improve the results of ref.[33] (particularly, for the K^* radiative decays) where such a source of SU(3)-breaking has been neglected. As mentioned, the other SU(3)-breaking parameter c_V is fixed here so as to satisfy the relation $M_\phi^2 = (1 + 2c_V)M_\rho^2$.

To enlarge our discussion, we have also tried to fit the radiative decays with a different set of parameters. The choice, which is shown in Table 4 was based on the use of the set $c_V = 0.28$ and $c_A = 0.36$, which was considered optimal in the previous section, when chiral loop contributions were added to the vector meson terms. Notice that because the use of eq.(88) would introduce an error in eqs.(89) for this value of c_V, we refrain from using it in the whole set of those equations, which now come to depends explicitly upon the parameter c_V. On its turn, this means that the whole numerical dependence of those equations upon the parameters c_A and c_{WZ} changes and we obtain a different set of optimal values, which are in line with the results of refs. [33] and [2], and shown in last column of Table 4. Again the agreement is quite good and the decision of how to optimize the use of our lagrangians remains open waiting for improved data and analysis.

In summary, well-known SU(3)-breaking effects have been shown to be easily introduced in effective lagrangians incorporating vector-mesons. In particular, the VVP interactions, related to radiative vector-meson decays – for which accurate new data are expected – and to the anomalous π, $\eta \to \gamma\gamma$ decays, are accurately described, improving the results of previous related work [33].

References

[1] U.-G. Meissner, Phys. Rep. 161 (1988) 213.

[2] M. Bando, T. Kugo and K. Yamawaki, Nucl. Phys. *B259* (1985) 493, and Phys. Rep. 164 (1988) 217.

[3] J. Gasser and H. Leutwyler, Nucl. Phys. *B250* (1985) 465, 517, 539.

[4] G. Ecker, J. Gasser, A. Pich and E. de Rafael, Nucl. Phys. *B321* (1989) 311.
J.F. Donoghue, C. Ramirez and G. Valencia, Phys. Rev. *D39* (1989) 1947.

[5] J. Bijnens, Int. J. Mod. Phys. *A8* (1993) 3045 and references therein.

[6] Ll. Ametller, J. Bijnens, A. Bramon and F. Cornet, Phys. Rev. D45 (1992) 986.

[7] CELLO Collaboration, *Z. Phys.***C 49** (1991) 401.

[8] M.R. Pennington and J. Portolés, preprint DTP-94/54 and Phys. Lett. (in press).

[9] A. Bramon, A. Grau and G. Pancheri, Phys. Lett. *B317* (1993) 190.

[10] D. Kalafatis, private communication.

[11] J.J. Sakurai, *Currents and Mesons*, University of Chicago, Chicago 1969.

[12] J. Bijnens, A. Bramon and F. Cornet, *Z. Phys.***C 46** (1990) 599.

[13] *Particle Data Group*, Phys. Rev. *D45* (1992) 1.

[14] T. Fujiwara et al., *Progr. Theor. Phys.***73** (1985) 926.

[15] A. Bramon, E. Pallante and R. Petronzio, Phys. Lett. *B271* (1991) 237.

[16] A. Bramon, A. Grau, E. Pallante, G.Pancheri and R. Petronzio, "The Effective Photon-Pseudoscalar Anomalous Interactions : $e^+e^- \to \pi^+\pi^-\pi^0, \pi^0\gamma, \eta\gamma, \pi^0\gamma^*$", The DAΦNE Physics Handbook, pag. 305, Vol.II. Eds. L. Maiani et al. INFN, Frascati September 1992.

[17] R.I. Dzhelyadin et al., *Phys. Lett.* **B102** (1981) 296.

[18] M. Crisafulli and V. Lubicz, "Electromagnetic decays of vector mesons in lattice QCD", The DAΦNE Physics Handbook, pag. 499, Vol.II. Eds. L. Maiani et al. INFN, Frascati September 1992.

[19] E. Pallante and R. Petronzio, Phys. Lett. B292 (1992) 143.

[20] S.I.Dolinsky et al., Phys. Rep. 202 (1991) 99.

[21] A. Bramon, A. Grau and G. Pancheri, Phys. Lett. B283 (1992) 416.

[22] S.Fajfer and R.J.Oakes, Phys. Rev. D42 (1990) 2392.

[23] F.M.Renard, Nuovo Cim. 62A (1969) 475.

[24] N.N.Achasov and V.N.Ivanchenko, Nucl Phys. B315 (1989) 465.

[25] P.Singer, Phys. Rev. 128 (1962) 2789; 130 (1963) 2441; 161 (1967) 1694(E).

[26] A. Bramon, A. Grau and G.Pancheri "Vector Meson and Chiral Loops Contributions to the decays $V^0 \to P^0 P^0 \gamma$", The DAΦNE Physics Handbook, pag. 467, Vol.II. Eds. L. Maiani et al. INFN, Frascati September 1992.

[27] S.Nussinov and T.N.Truong, Phys. Rev. Lett. 63 (1989) 2003.

[28] J.L.Lucio M. and J.Pestieau, Phys. Rev. D42 (1990) 3253.

[29] N.Paver and Riazuddin, Phys. Lett. B246 (1990) 240.

[30] A. Quenzer et al., Phys. Lett. B76 (1977) 512. E.B. Dally et al., Phys. Rev. Lett. 39 (1977) 1176. E.B. Dally et al., Phys. Rev. Lett. 48 (1982) 375. S.R. Amendolia et al., Phys. Lett. B178 (1986) 435. W.R. Molzon et al., Phys. Rev. Lett. 41 (1978) 1231. C. Erkal and M.G. Olsson, J. Phys. G: Nucl. Phys. 13 (1987) 1355.

[31] A. Bramon, A. Grau and G. Pancheri, Phys. Lett. B345 (1995) 263.

[32] A. Sirlin, Phys. Rev. Lett. 43 (1979) 904; Ann. Phys.(N.Y.) 61 (1970) 294.

[33] O. Hajuj, Z. Phys. C 60 (1993) 357.